UNIVERSITY OF Southampton

Linear Vibration Energy Harvesting

Dr. Bahareh Zaghari

Smart Electronic Materials and Systems Research Group
Electronics and Computer Science
University of Southampton, UK

bahareh.zaghari@soton.ac.uk

NiPS Summer School
July 17-20, 2018
Perugia, Italy

These slides are available on GitHub at https://tinyurl.com/y9uwtz3q.

Energy harvesting components

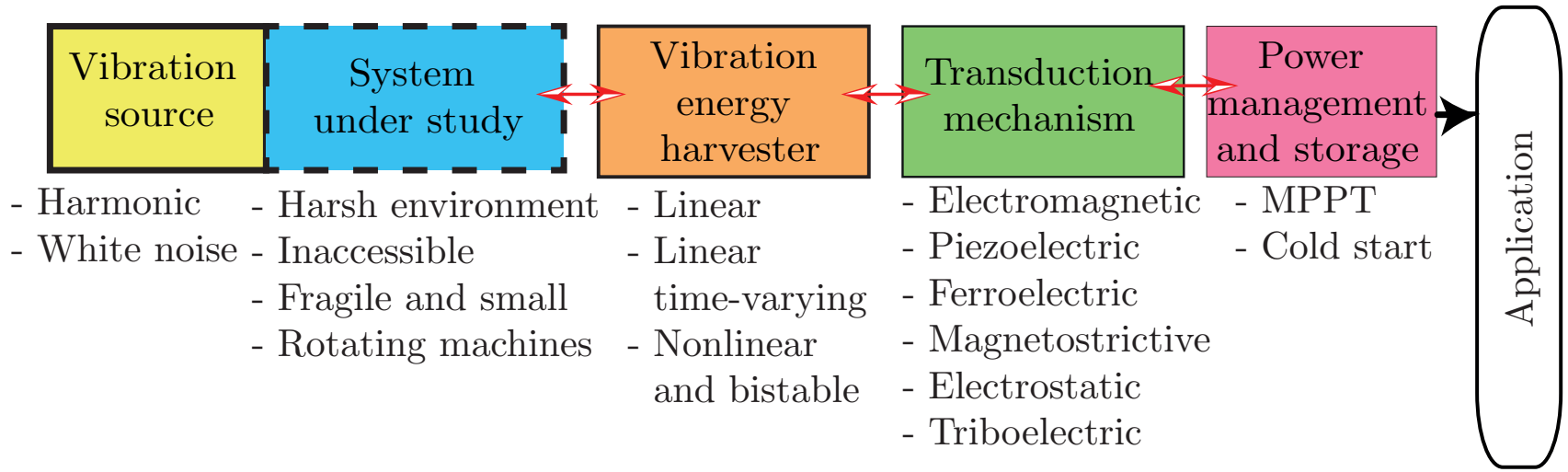

All above contribute to

$$\text{Efficiency} = \frac{\text{Input energy}}{\text{Output energy}}$$

Relevant references

- R. S. Langley, A general mass law for broadband energy harvesting
- S. Roundy, On the Effectiveness of Vibration-based Energy Harvesting
- K. Nakano et al., A unified approach to optimal conditions of power harvesting using electromagnetic and piezoelectric transducers
- C. Cepnik et al., Approaches for a Fair Comparison and Benchmarking of Electromagnetic Vibration Energy Harvesters

Why energy harvesting?

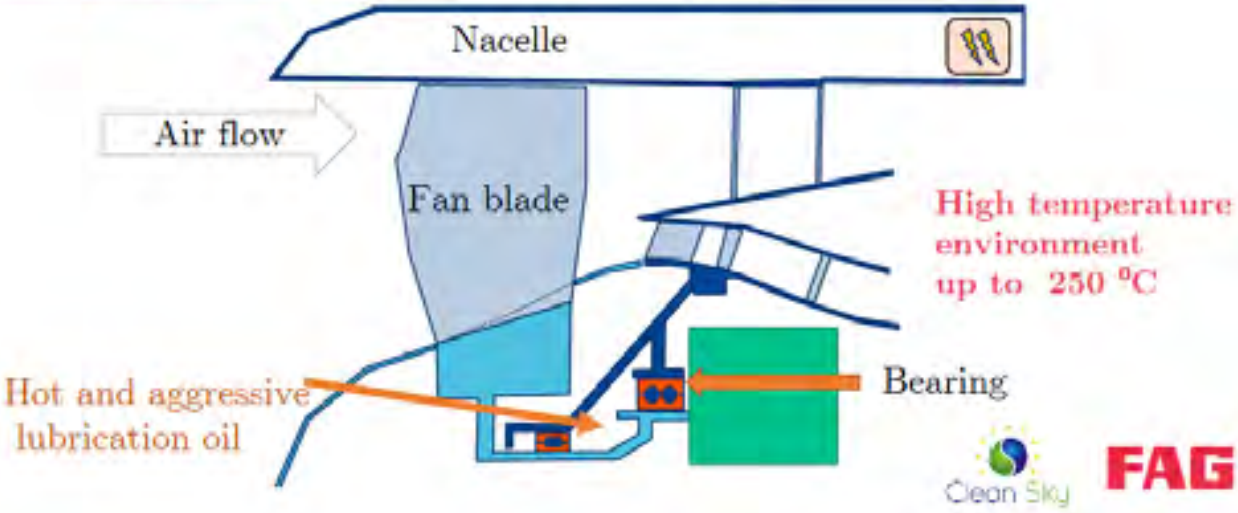

Future of aerospace wireless sensor network

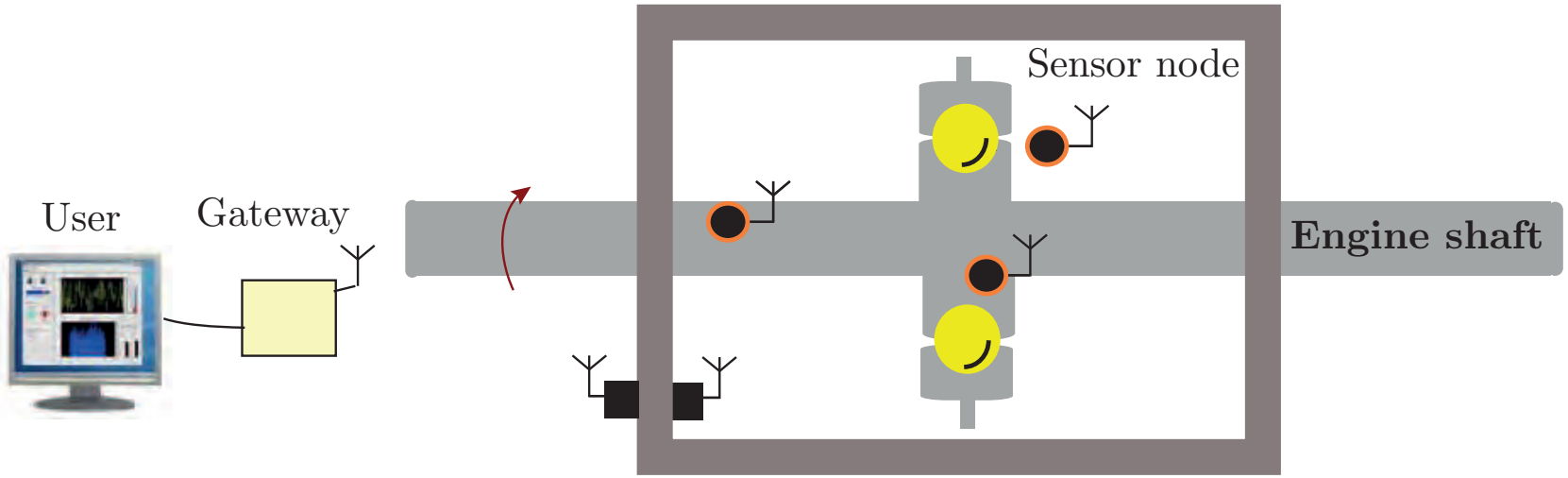

Ball bearing schematic as
part of the jet engine

Objective: To develop a **smart system** incorporating

multiple sensors, energy harvesting, wireless communications, and data analytics

for **intelligent monitoring** of aero-engines.

Future of aerospace wireless sensor network

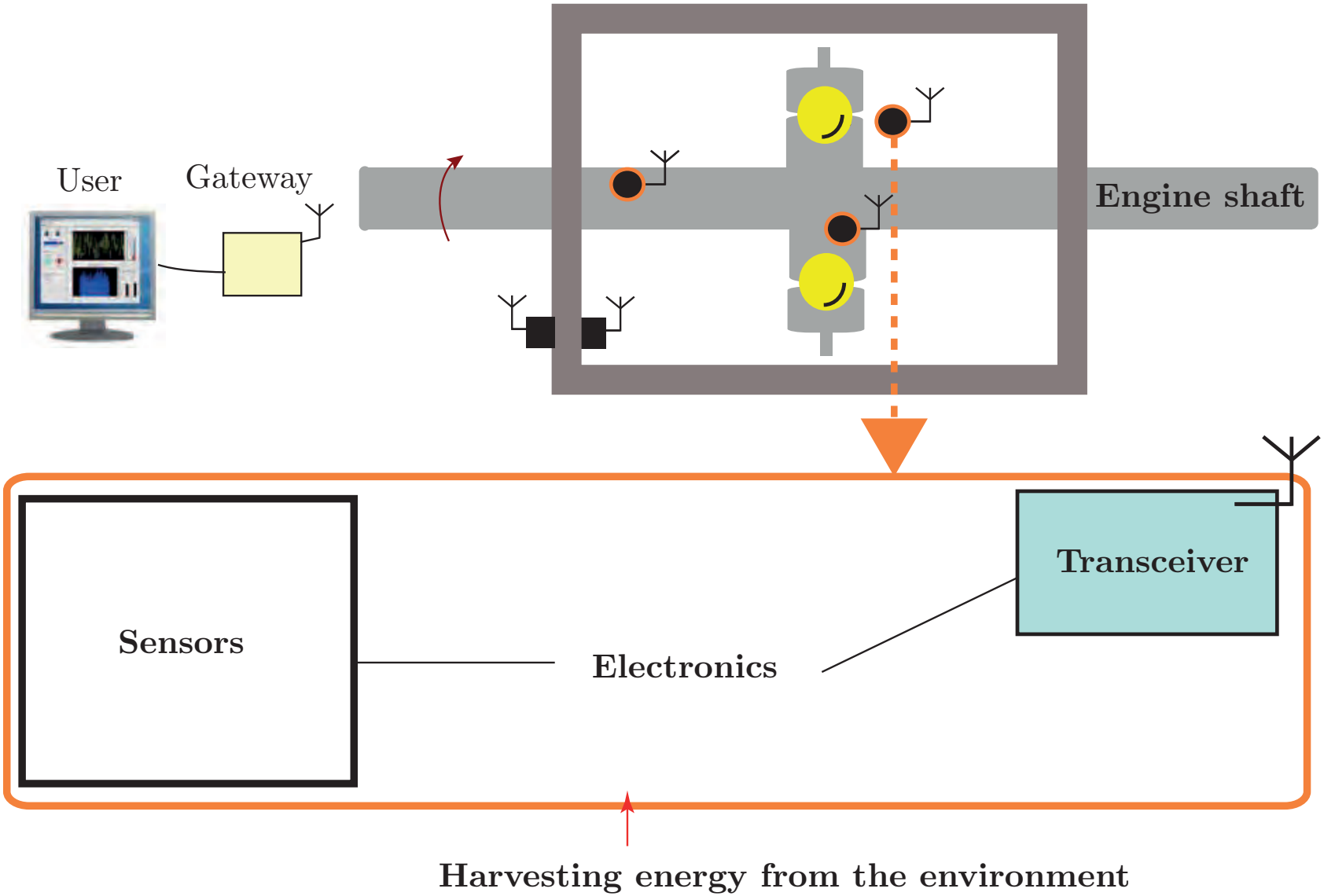

Future of aerospace wireless sensor network

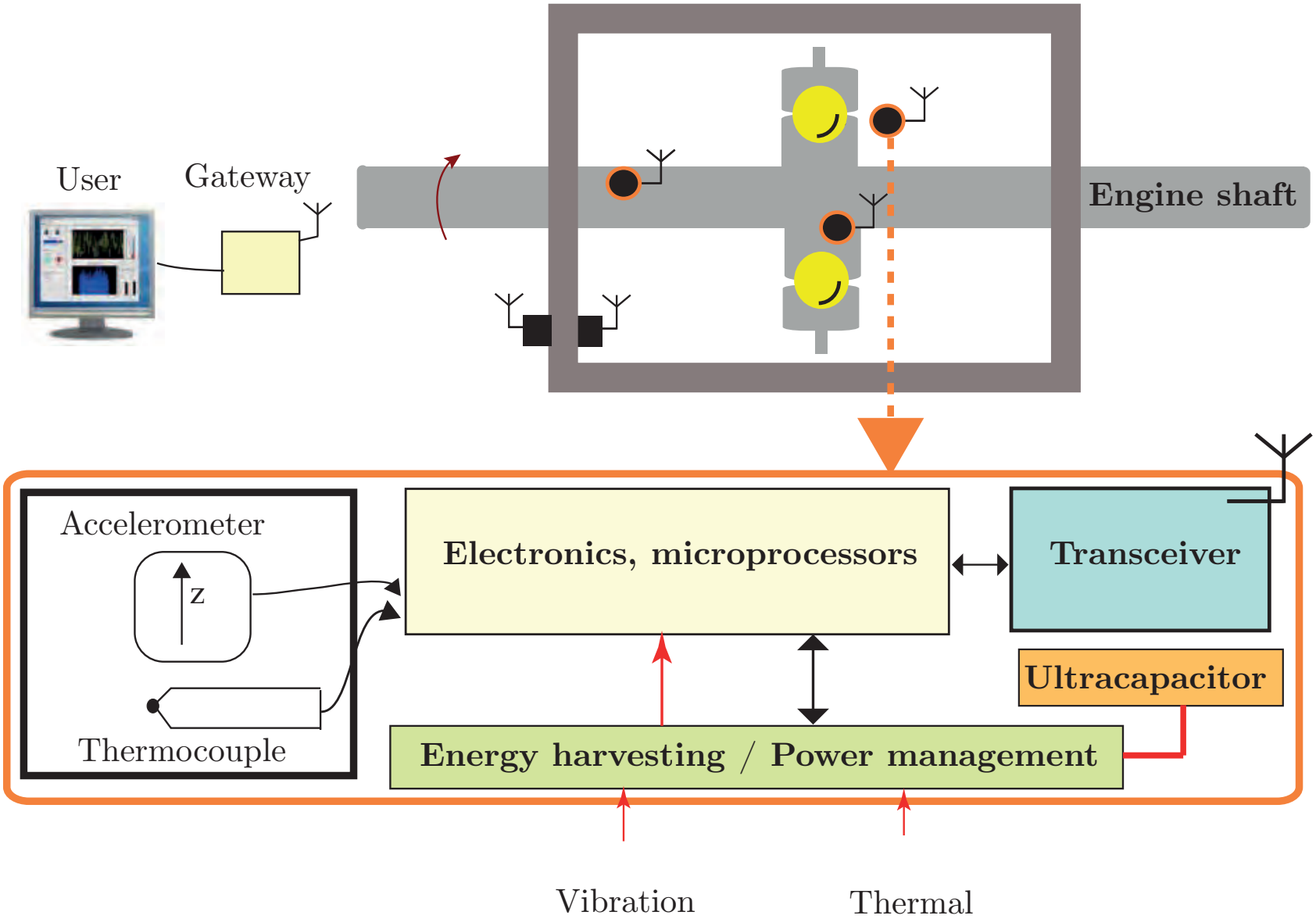

Industrial applications and challenges

- Existence of range of frequencies.
- Vibration levels can be very low (<25 mg).
- Reliable operation is required over many years.
- Operate across wide temperature ranges.

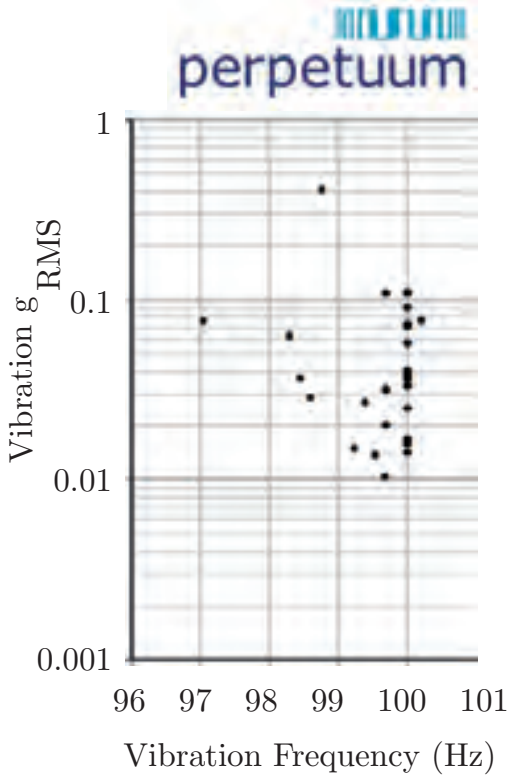

(a)

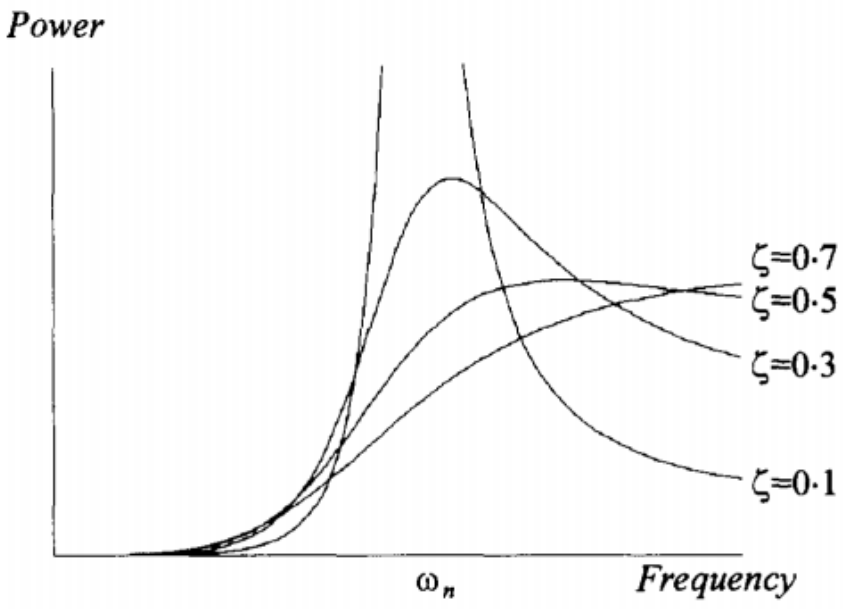

(b)

(a) Vibration data from AC motors at UK Waterworks. (b) Wiliams and Yates, 1996.

Industrial applications and challenges

perpetuum

Harvester bandwidth optimized to deliver 0.3mW from 95% of industrial AC motors with no adjustment. Maximum power output 50 mW.

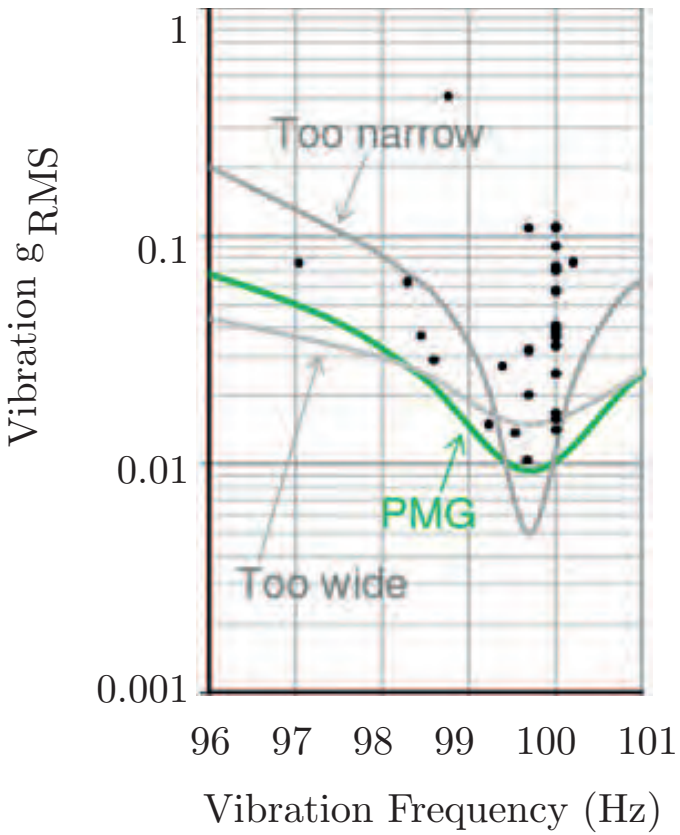

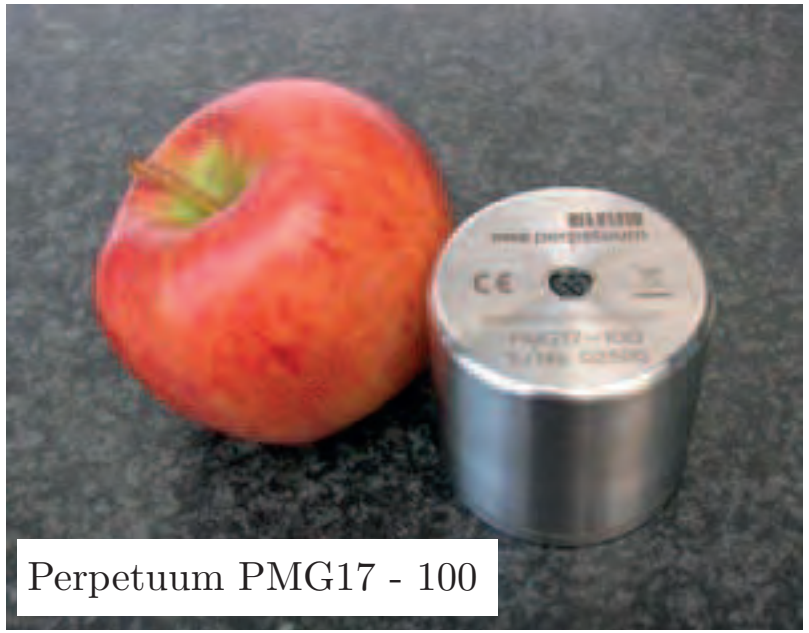

Temperature stability

Mechanical resonators can drift with temperature changes. Without considering the stabilisation, harvesters can stop working when the temperature is different.

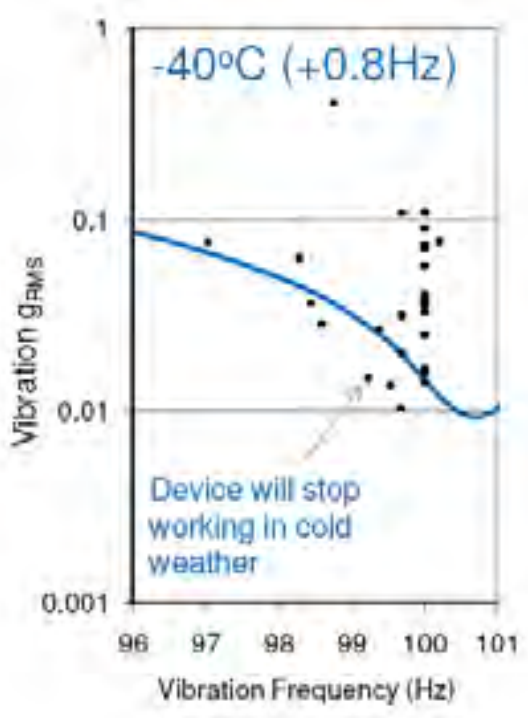

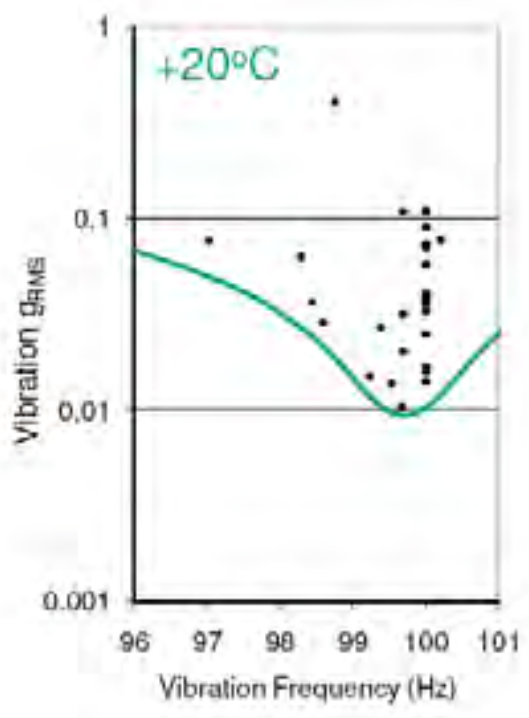

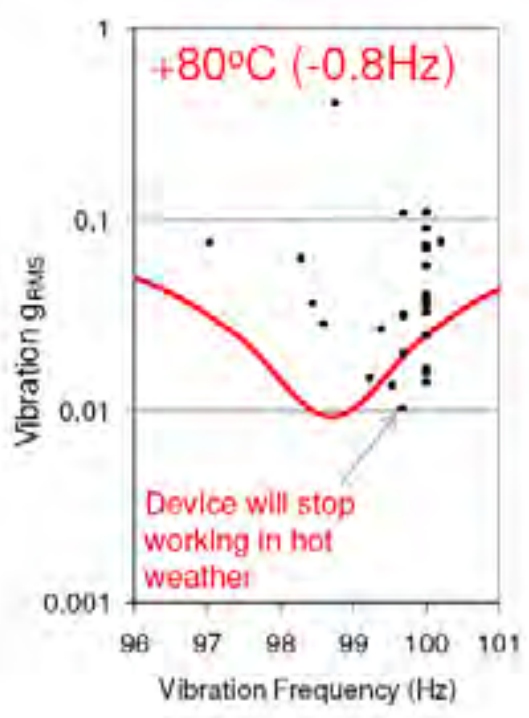

PMG17 temperature stability

The PMG17 has a temperature compensated resonator keeping the centre frequency fixed to within +/- 0.1 Hz over the full industrial temperature range.

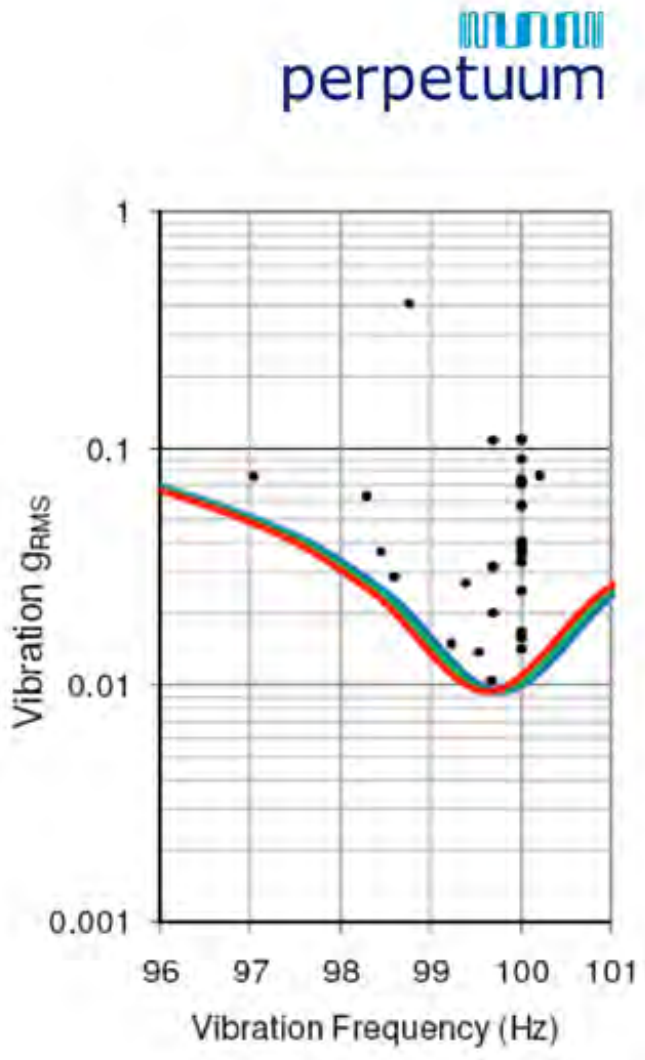

A simple electromagnetic energy harvester

- Cantilever electromagnetic harvester
- Tunable between 44-60Hz
- Packaged size: 0.8cm^3, 1.6g
- Power = 58mW at 1.12V at max input accelerations of 0.6ms^{-2}
- 51% of mechanical energy converted into electrical

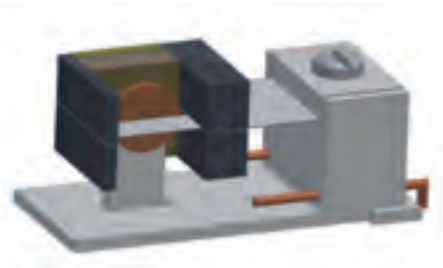

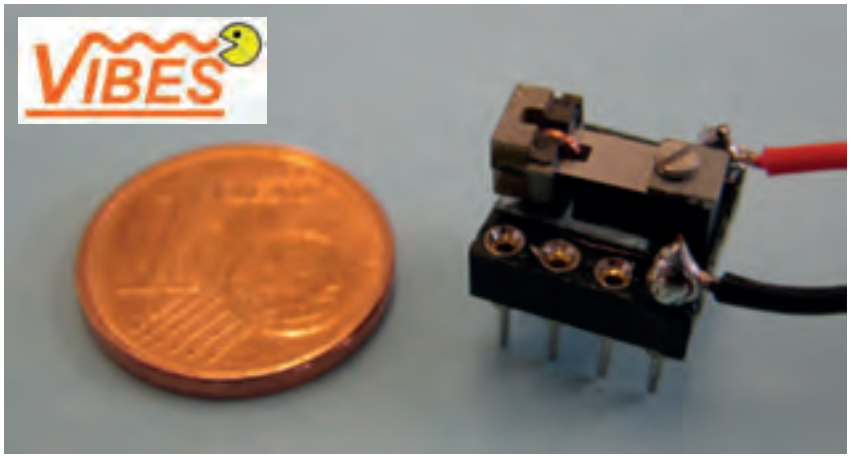

S. P. Beeby, 2007

Basic considerations for a linear energy harvester

Mechanical energy stored in the generator is

$$P_{\text{av}} = \frac{m\omega_{\text{n}}^3 X^2}{4\zeta}, \tag{1}$$

m is the inertial mass, ω_{n} is the natural frequency, X is external vibration displacement, and the damping ratio $\zeta = \dfrac{c}{2m\omega_{\text{n}}}$.

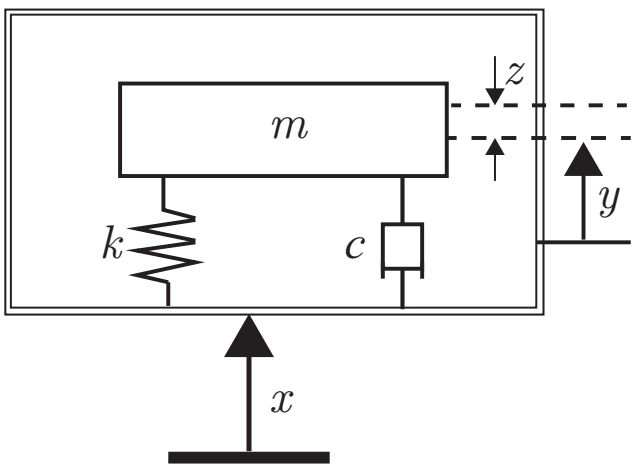

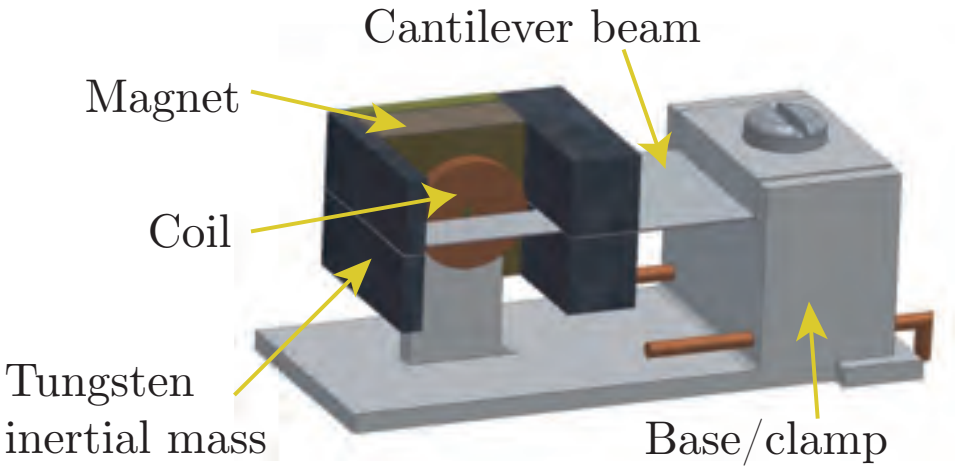

S. P. Beeby, 2007

Linear time-varying systems

(a)

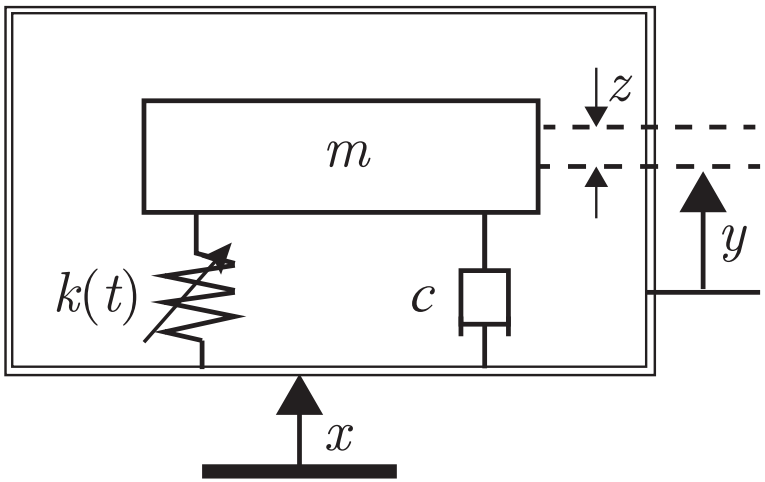

$$x = X\cos(\omega t + \phi)$$

$$m\ddot{z} + c\dot{z} + k(t)z = -m\ddot{x}$$
$$k(t) = k_c + k_p\cos(\Omega t)$$

(b)

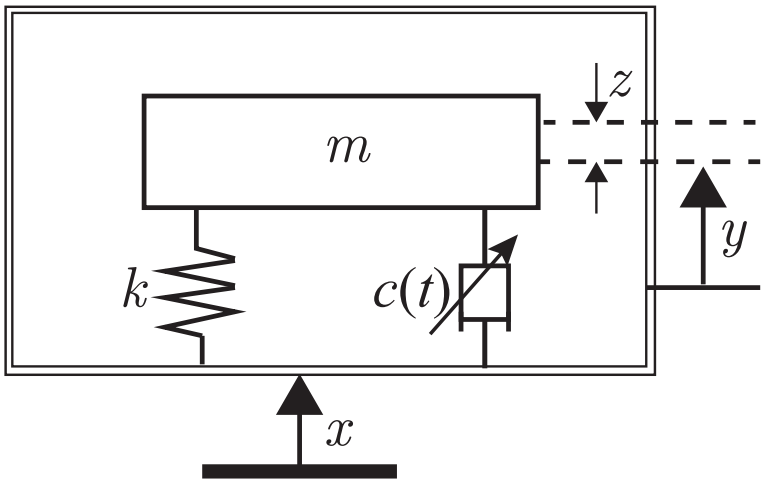

$$x = X\cos(\omega t)$$

$$m\ddot{z} + c(t)\dot{z} + kz = -m\ddot{x}$$
$$c(t) = c_0 + c_p\cos(\Omega t)$$

These systems have been exploited for vibration energy harvesting. (a) B. Zaghari et al., 2014. (b) M. Scapolan et al., 2017.

Examples of parametrically excited systems with time-periodic parameters

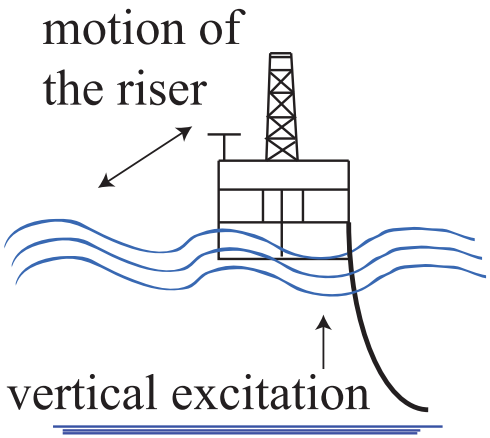

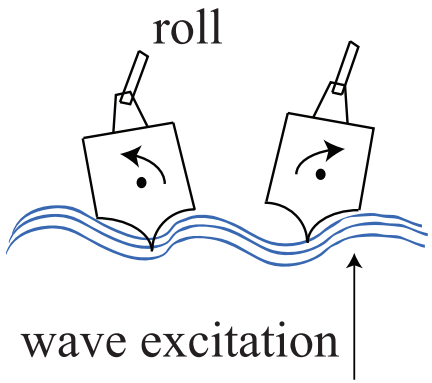

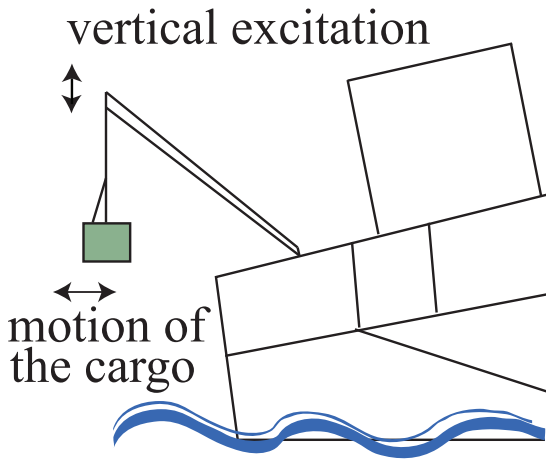

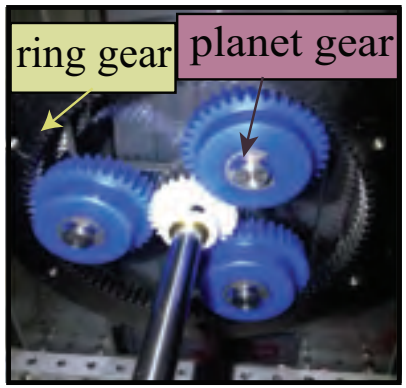

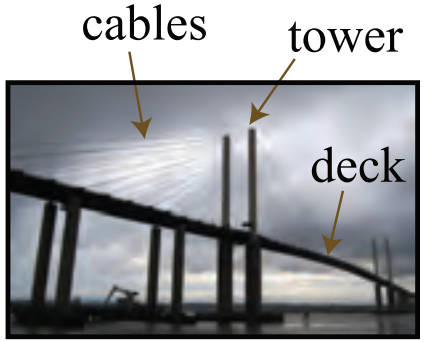

Queen Elizabeth II
Dartford, England

History repeats itself

The first people introduced and studied linear time-varying systems:

- Michael Faraday (1791-1867)
- Franz Melde (1832-1901)
- John William Strutt, 3rd Baron Rayleigh (1842-1919)
- Émile Léonard Mathieu (1835-1890)

Linear energy harvesters with time-varying parameters

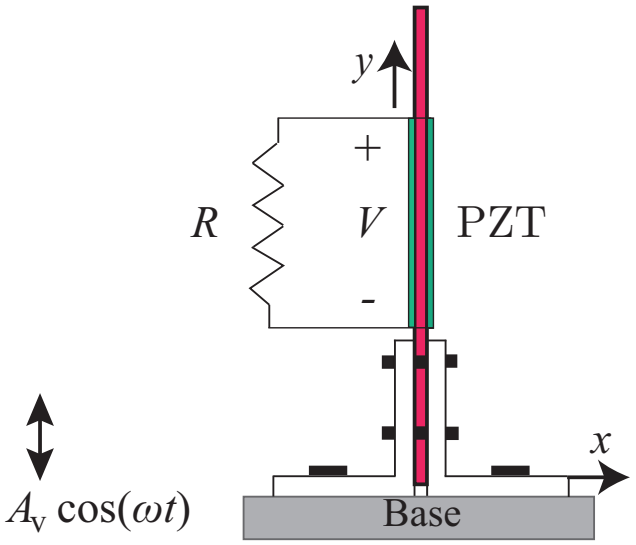

(a)

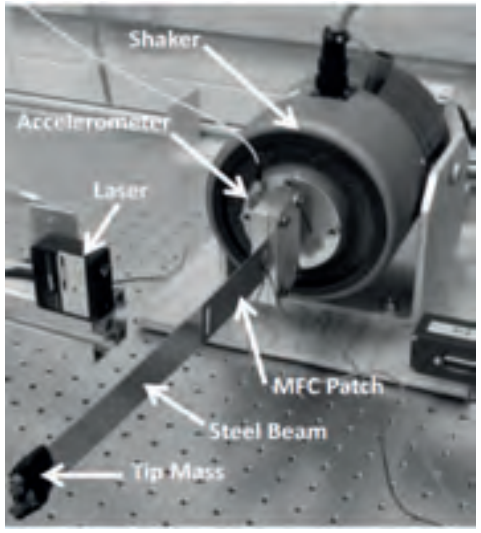

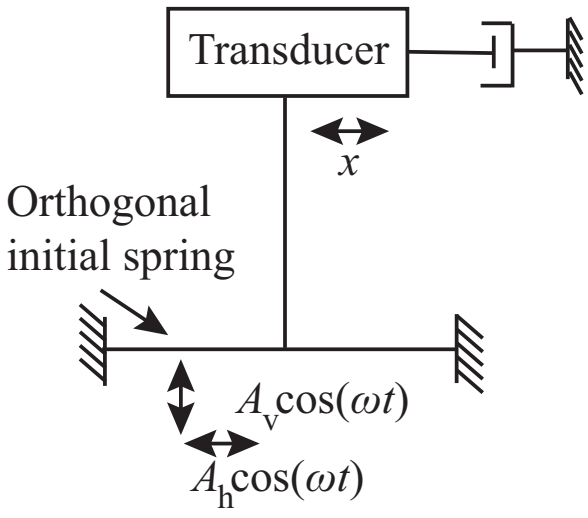

(b)

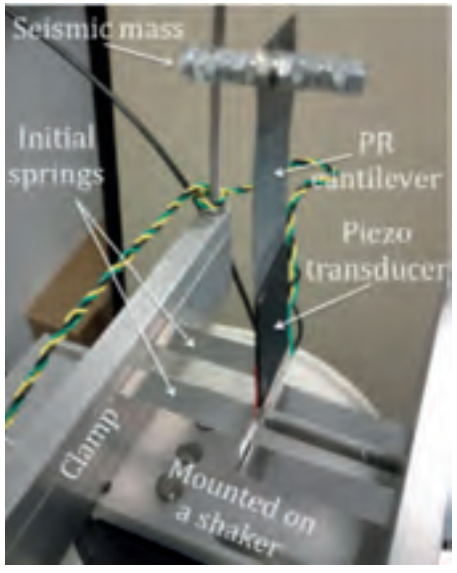

(a) M. Daqaq et al., 2008. (b) Y. Jia et al., 2014.

Modified Mathieu equation

$$\ddot{z} + 2\,\zeta\,\omega_n\,\dot{z} + \omega_n^2\left(1 + \delta\cos(\Omega\,t)\right)z = 0$$

- damping ratio

Modified Mathieu equation

$$\ddot{z} + 2\,\zeta\,\omega_n\,\dot{z} + \omega_n^2\left(1 + \delta\cos(\Omega\,t)\right)z = 0$$

- damping ratio
- natural frequency

Modified Mathieu equation

$$\ddot{z} + 2\,\zeta\,\omega_n\,\dot{z} + \omega_n^2\left(1 + \delta\cos(\Omega\,t)\right)z = 0$$

- damping ratio
- natural frequency
- parametric amplitude

Modified Mathieu equation

$$\ddot{z} + 2\,\zeta\,\omega_n\,\dot{z} + \omega_n^2\left(1 + \delta\cos(\Omega\,t)\right)z = 0$$

- damping ratio
- natural frequency
- parametric amplitude
- parametric frequency

Modified Mathieu equation

$$\ddot{z} + 2\,\zeta\,\omega_n\,\dot{z} + \omega_n^2\left(1 + \delta\cos(\Omega\,t)\right)z = 0$$

Stability and solutions of the Mathieu equation can be studied using:

- Floquet theory
- Method of Harmonic Balance (HBM)
- Perturbation methods (Methods of Averaging, Multiple Scales)

Unbounded solution

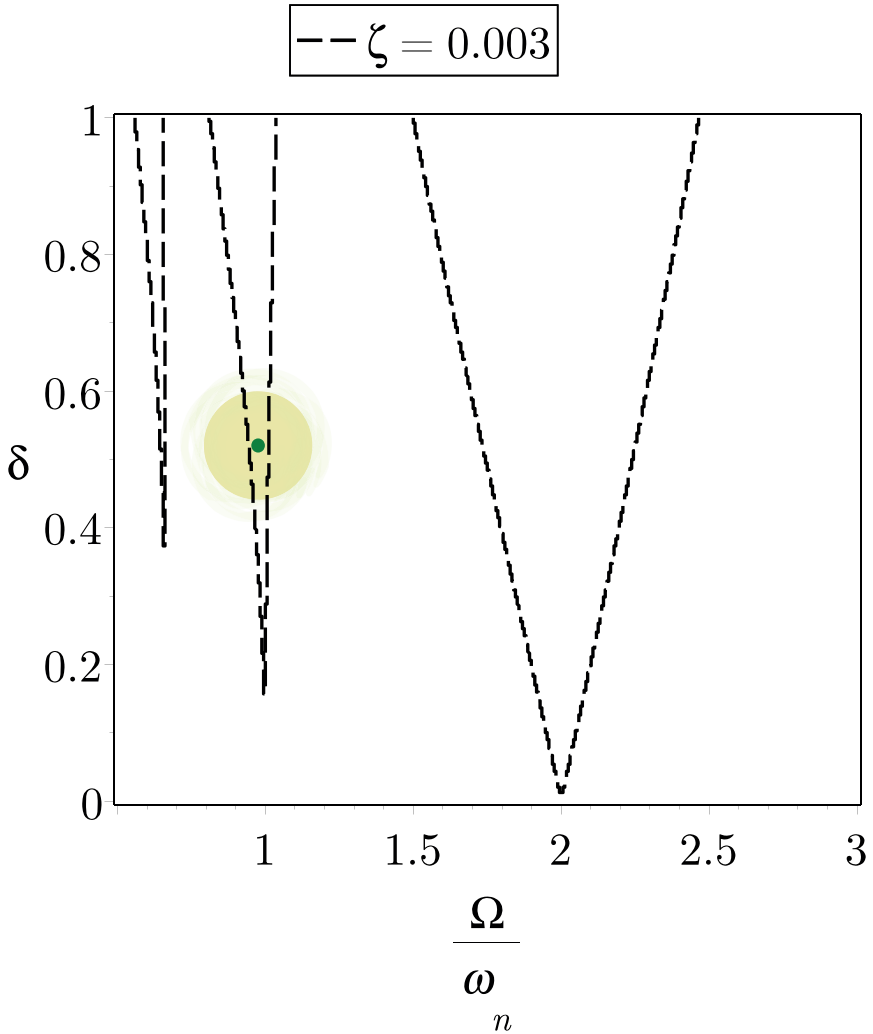

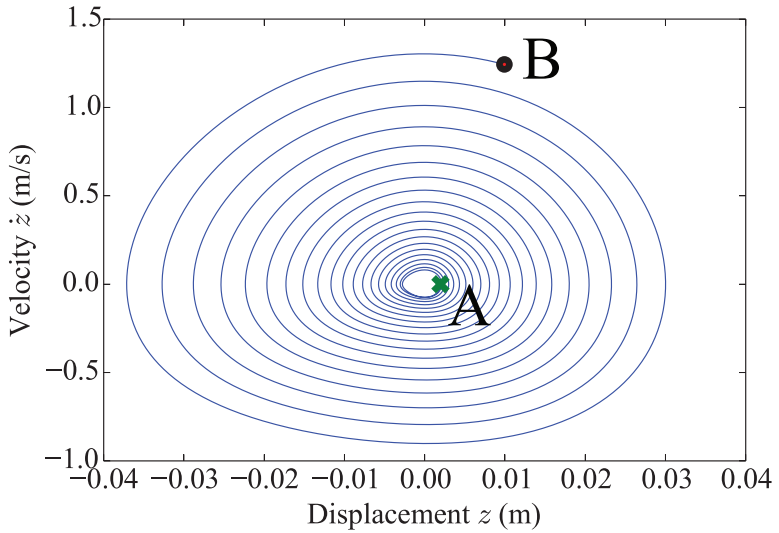

Strutt diagram with HBM and the numerical phase portrait for point $\delta = 0.5$ and $\frac{\Omega}{\omega_n} = 1$ is solved for 20 cycles (Initial condition: $z_0 = 0.002\text{m}$, $\dot{z}_0 = 0\text{ms}^{-1}$).

Limit cycle solution

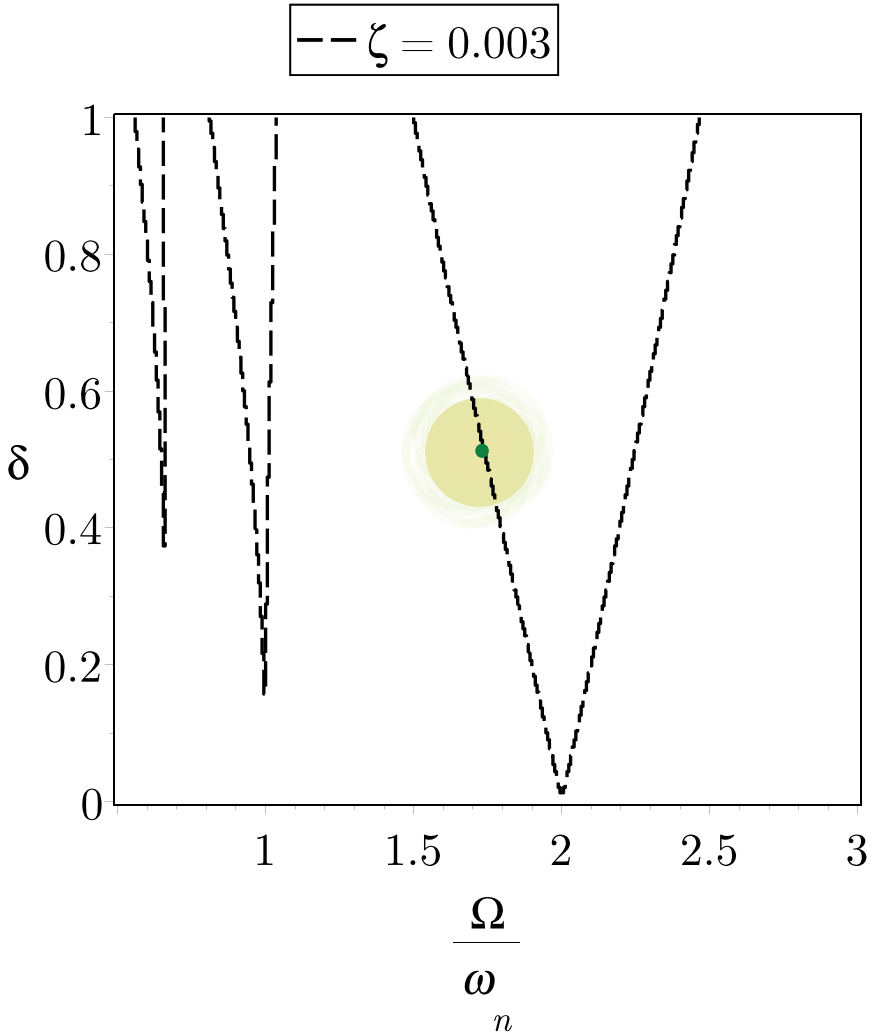

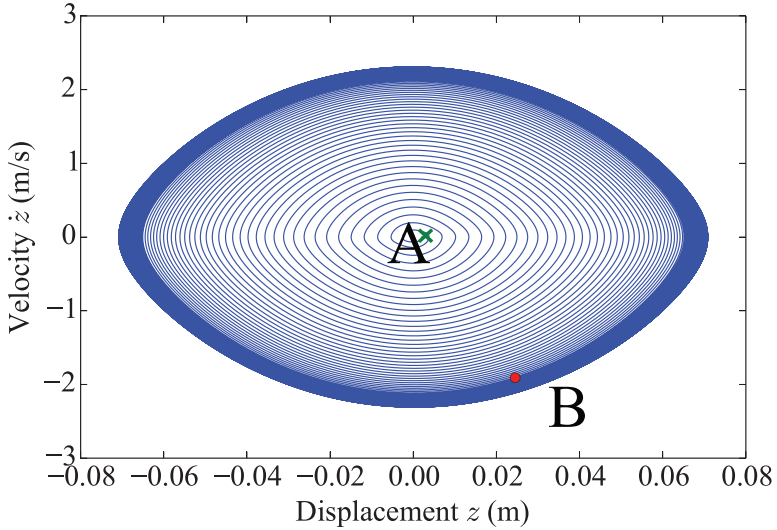

Strutt diagram with HBM and the numerical phase portrait for point $\delta = 0.5$ and $\frac{\Omega}{\omega_n} = 1.744$ is solved for 200 cycles (Initial condition: $z_0 = 0.002\text{m}$, $\dot{z}_0 = 0\text{ms}^{-1}$).

Unbounded solution

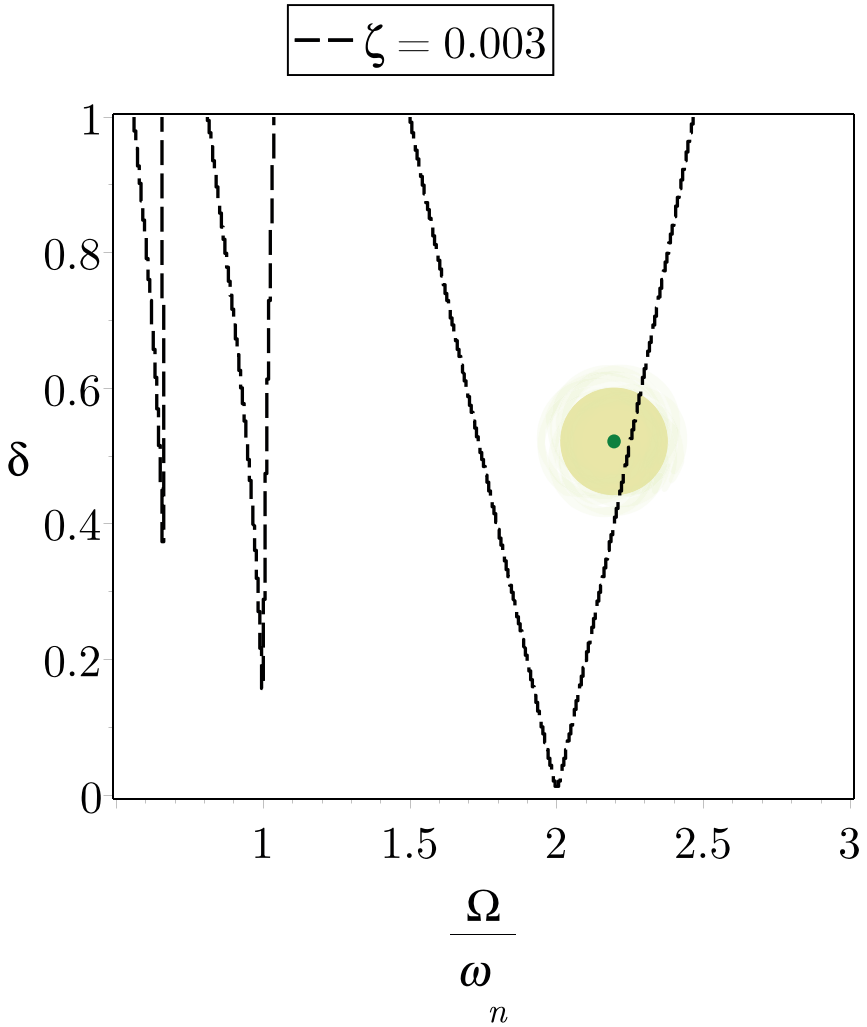

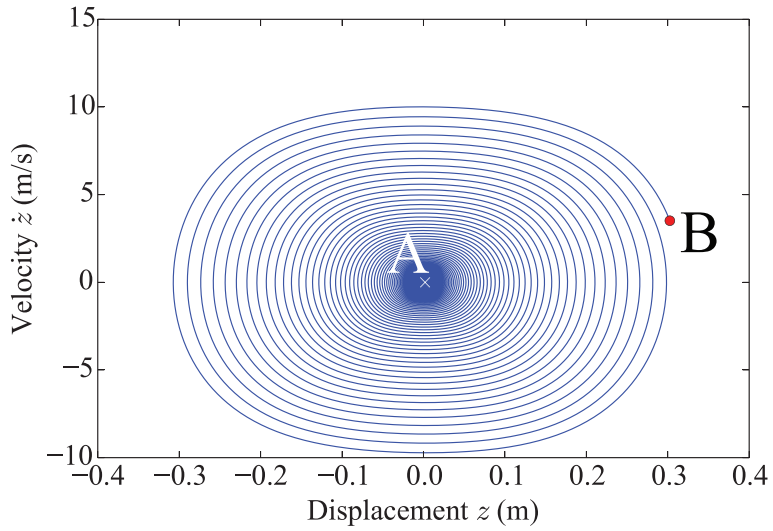

Strutt diagram with HBM and the numerical phase portrait for point $\delta = 0.5$ and $\frac{\Omega}{\omega_n} = 2.24$ is solved for 200 cycles (Initial condition: $z_0 = 0.002\text{m}$, $\dot{z}_0 = 0\text{ms}^{-1}$).

Bounded solution

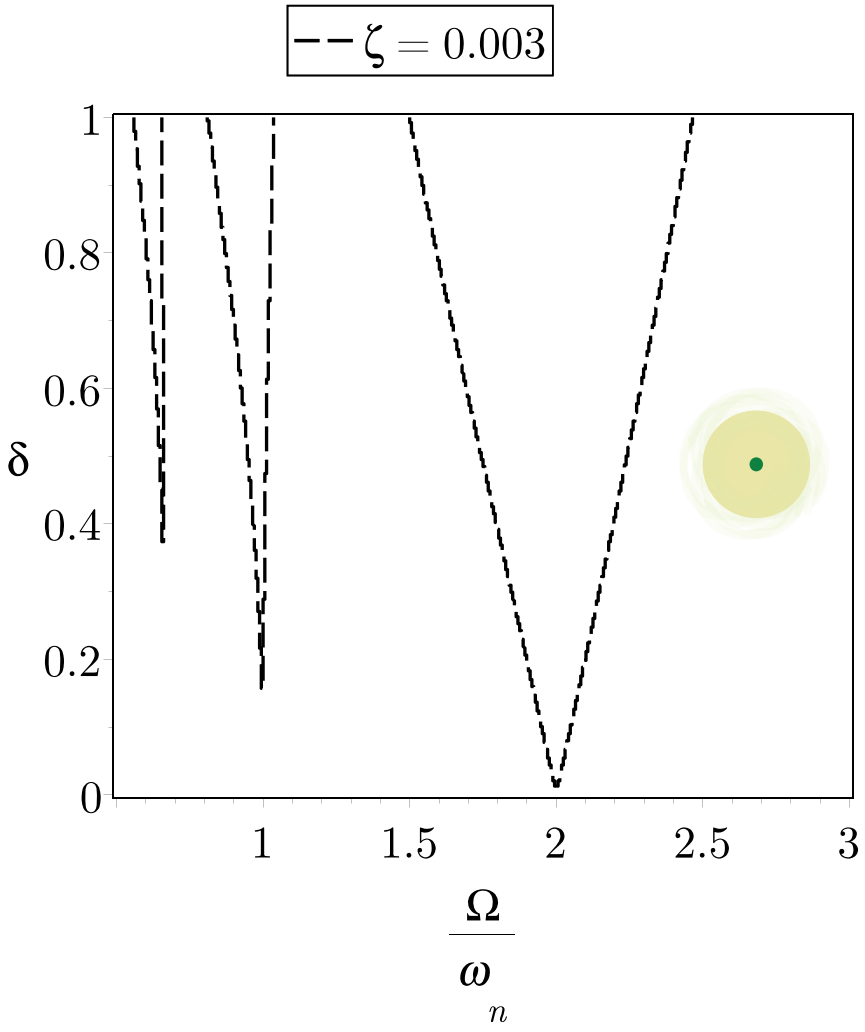

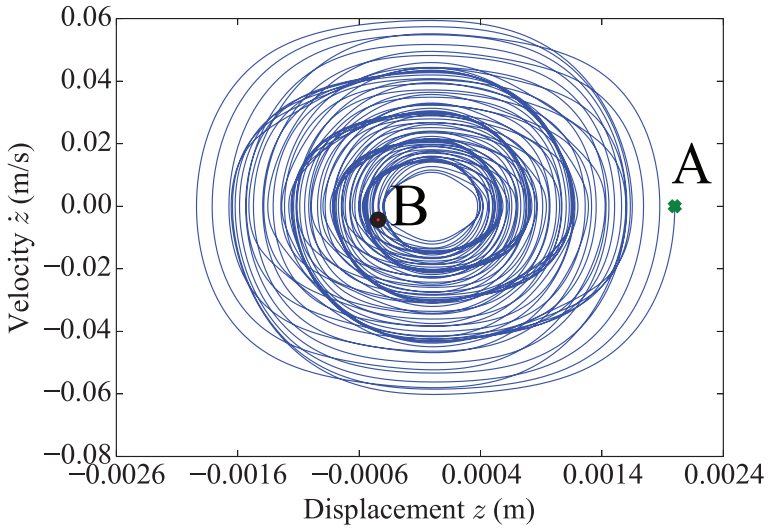

Strutt diagram with HBM and the numerical phase portrait for point $\delta = 0.5$ and $\frac{\Omega}{\omega_n} = 2.27$ is solved for 200 cycles (Initial condition: $z_0 = 0.002\text{m}$, $\dot{z}_0 = 0\text{ms}^{-1}$).

Effect of damping and instability thresholds

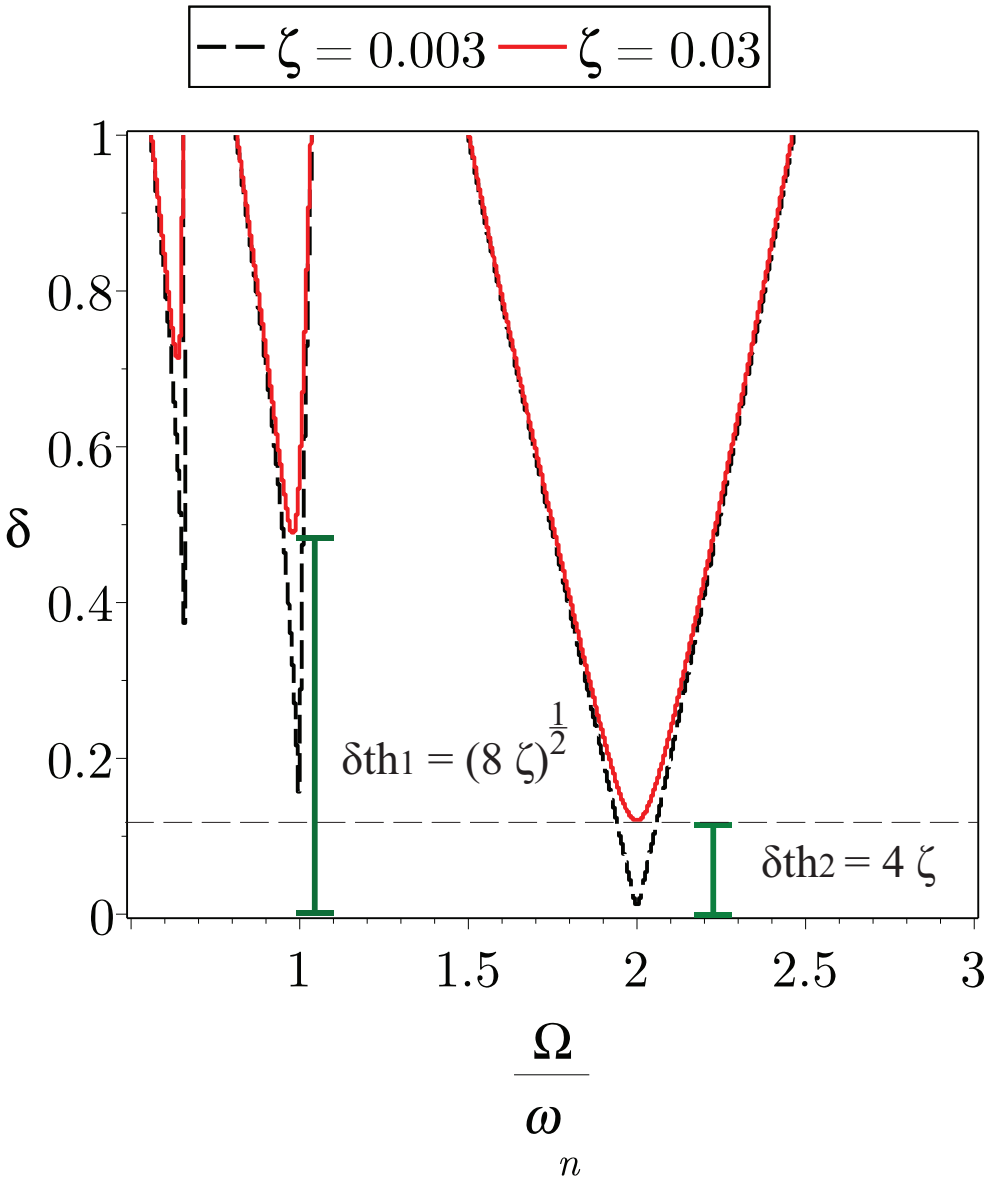

Reducing the instability threshold is beneficial for:

- parametrically excited vibration energy harvester
- parametrically excited amplifiers and filters

The effects of changing frequencies on response amplitude

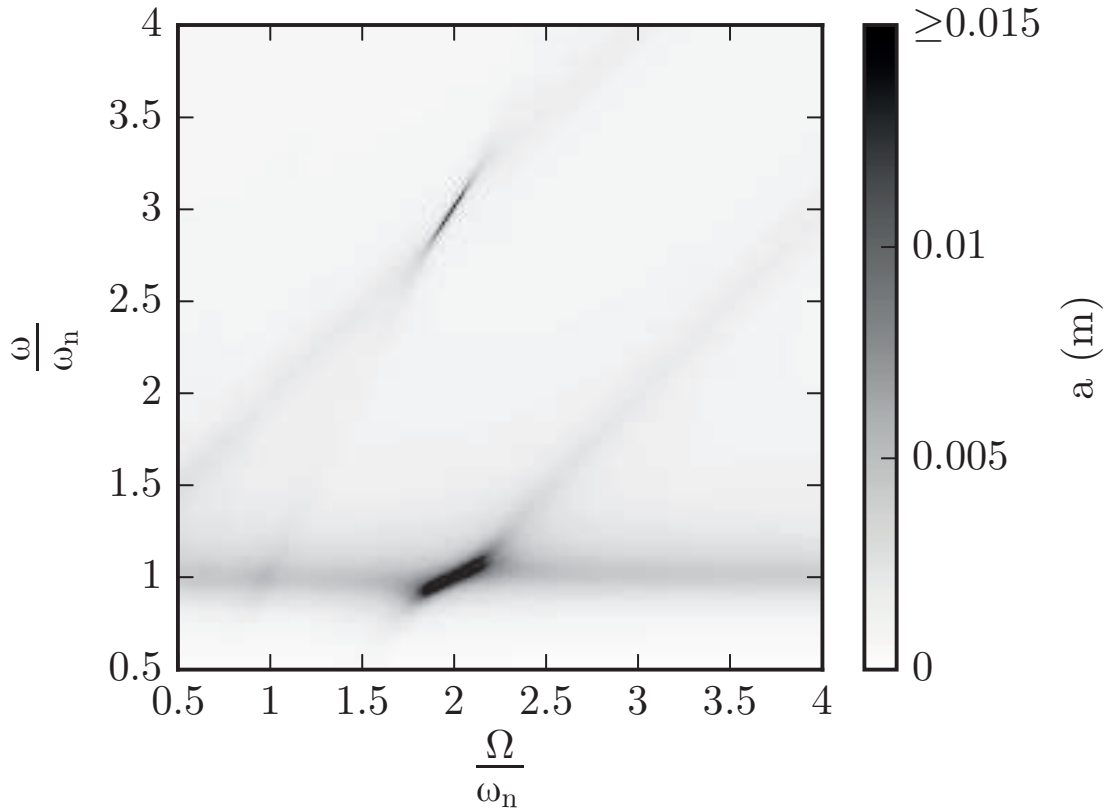

Maximum steady-state response amplitude a at different frequencies. $\delta = 0.4$, $\zeta = 0.1$, and base excitation amplitude is 0.001m (B. Zaghari, 2016)

The effects of changing frequencies on response amplitude

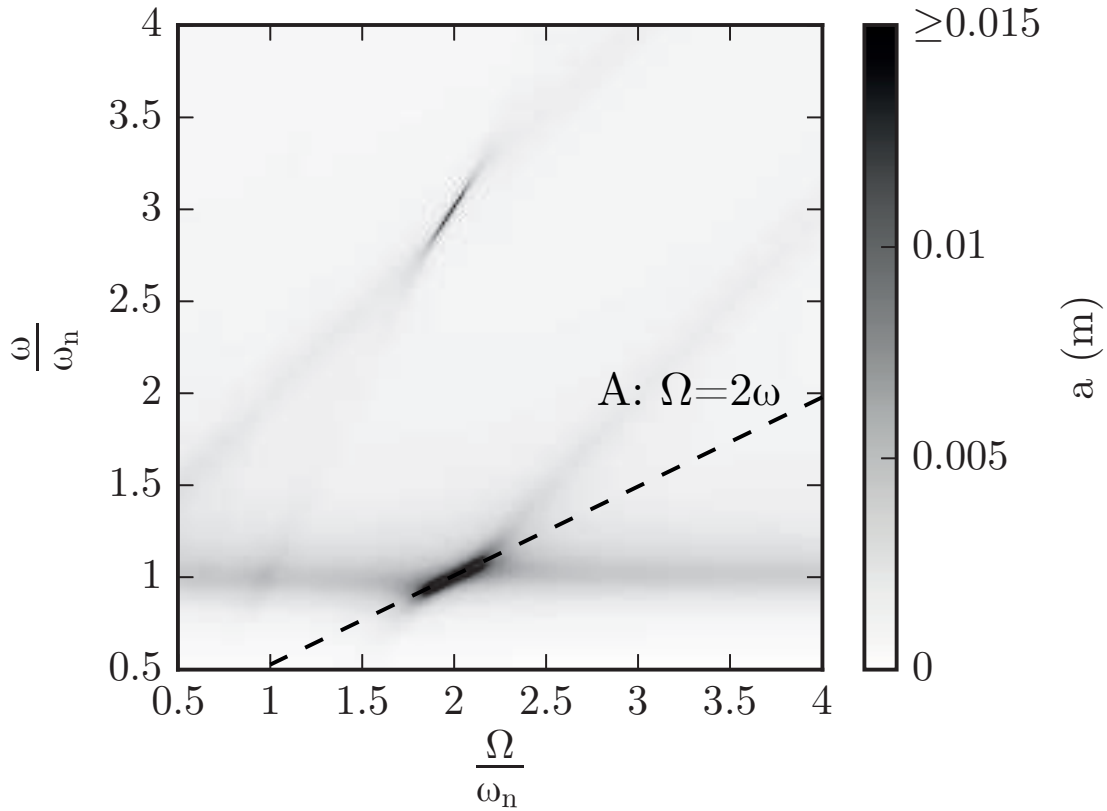

Maximum steady-state response amplitude a at different frequencies. $\delta = 0.4$, $\zeta = 0.1$, and base excitation amplitude is 0.001m (B. Zaghari, 2016)

The effects of changing frequencies on response amplitude

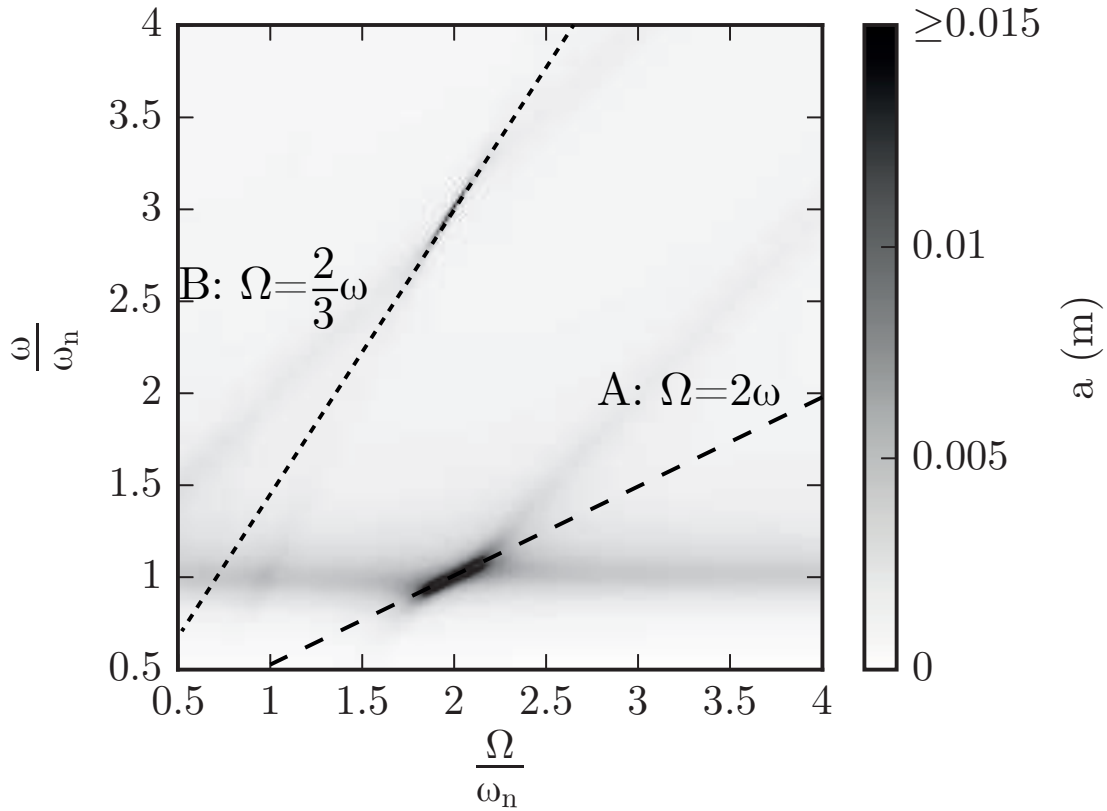

Maximum steady-state response amplitude a at different frequencies. $\delta = 0.4$, $\zeta = 0.1$, and base excitation amplitude is 0.001m (B. Zaghari, 2016)

The effects of changing frequencies on response amplitude

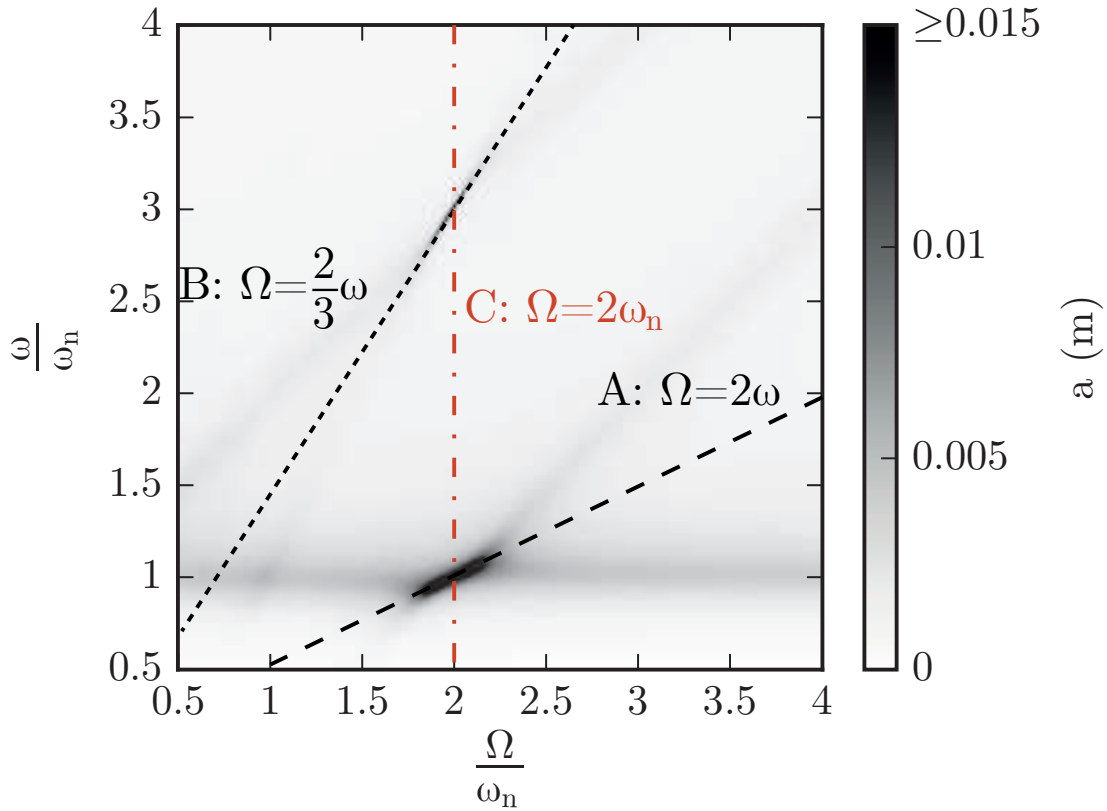

Maximum steady-state response amplitude a at different frequencies. $\delta = 0.4$, $\zeta = 0.1$, and base excitation amplitude is 0.001m (B. Zaghari, 2016)

The effects of changing frequencies on response amplitude

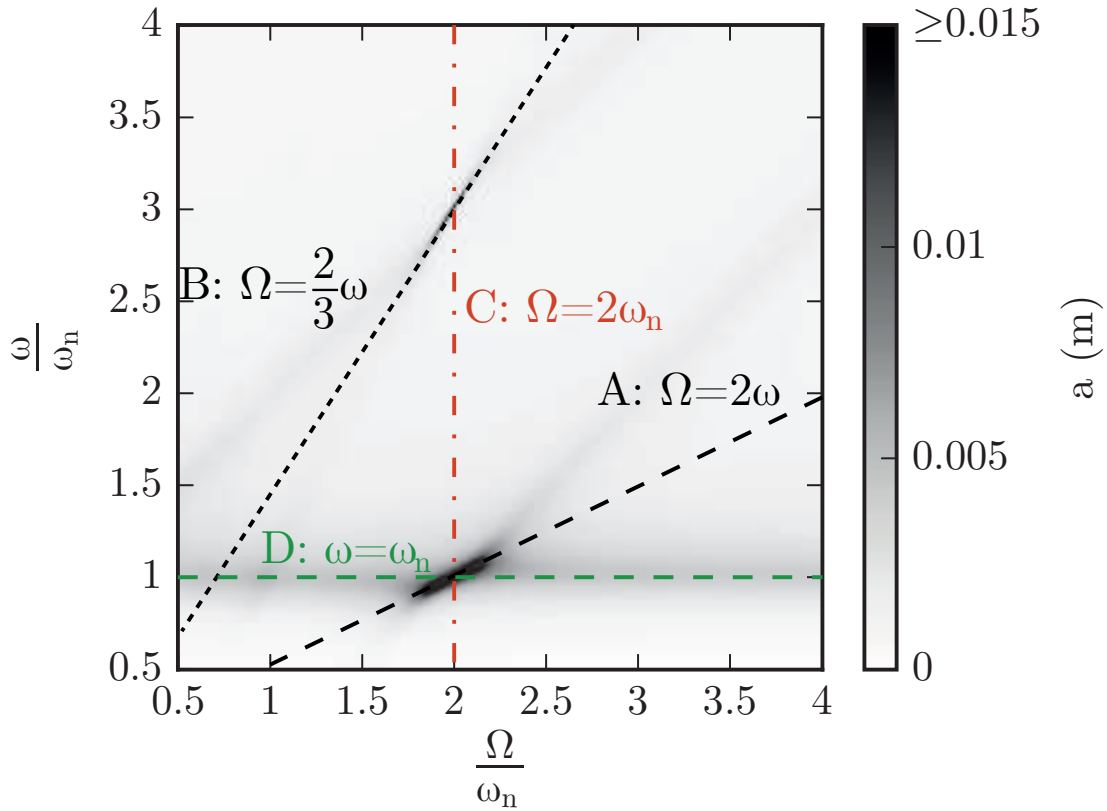

Maximum steady-state response amplitude a at different frequencies. $\delta = 0.4$, $\zeta = 0.1$, and base excitation amplitude is 0.001m (B. Zaghari, 2016)

The effects of changing frequencies on power consumption

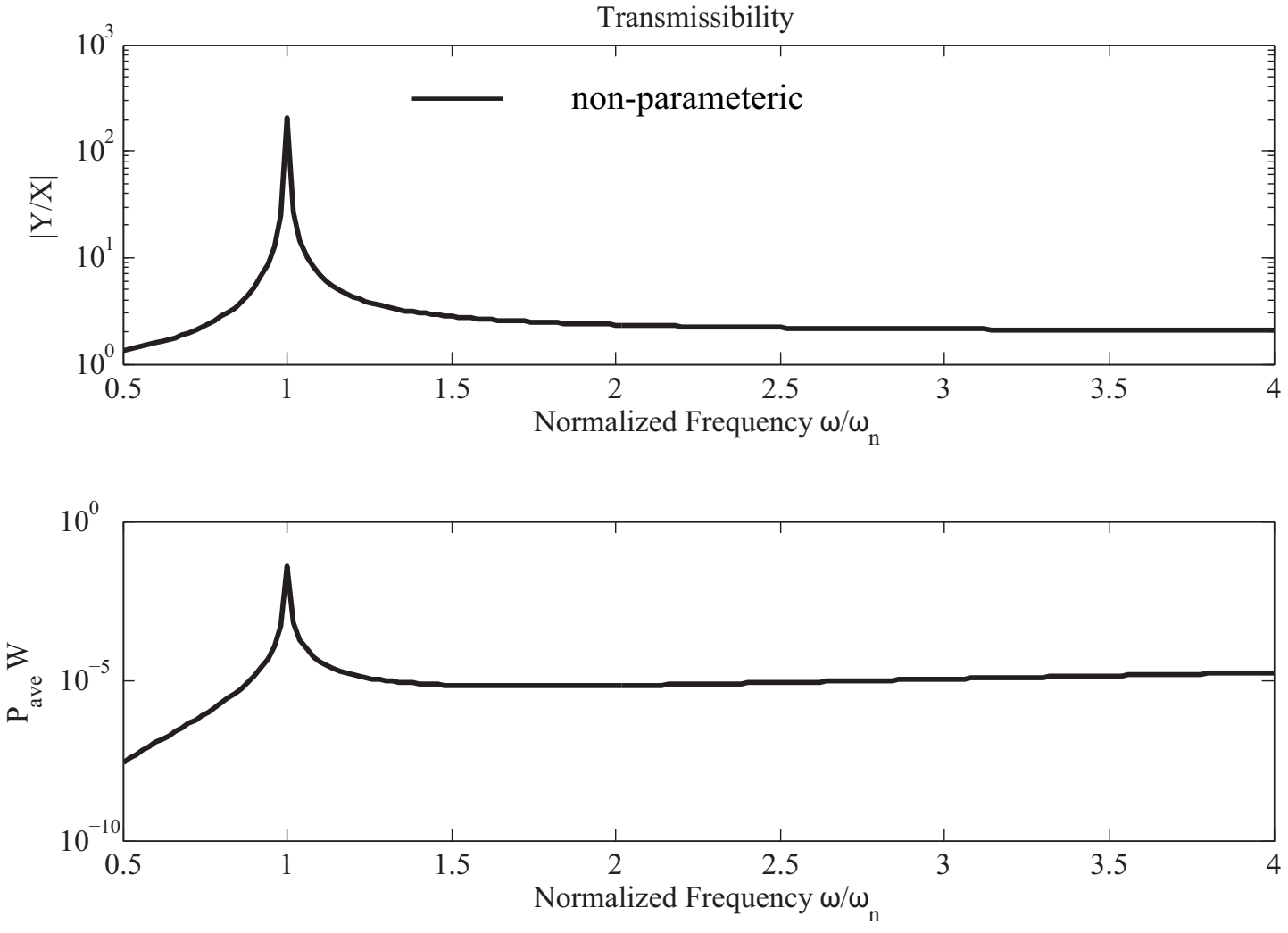

Analytical solutions of the non-parametric and parametric harvesters (B. Zaghari et al., 2014).

The effects of changing frequencies on power consumption

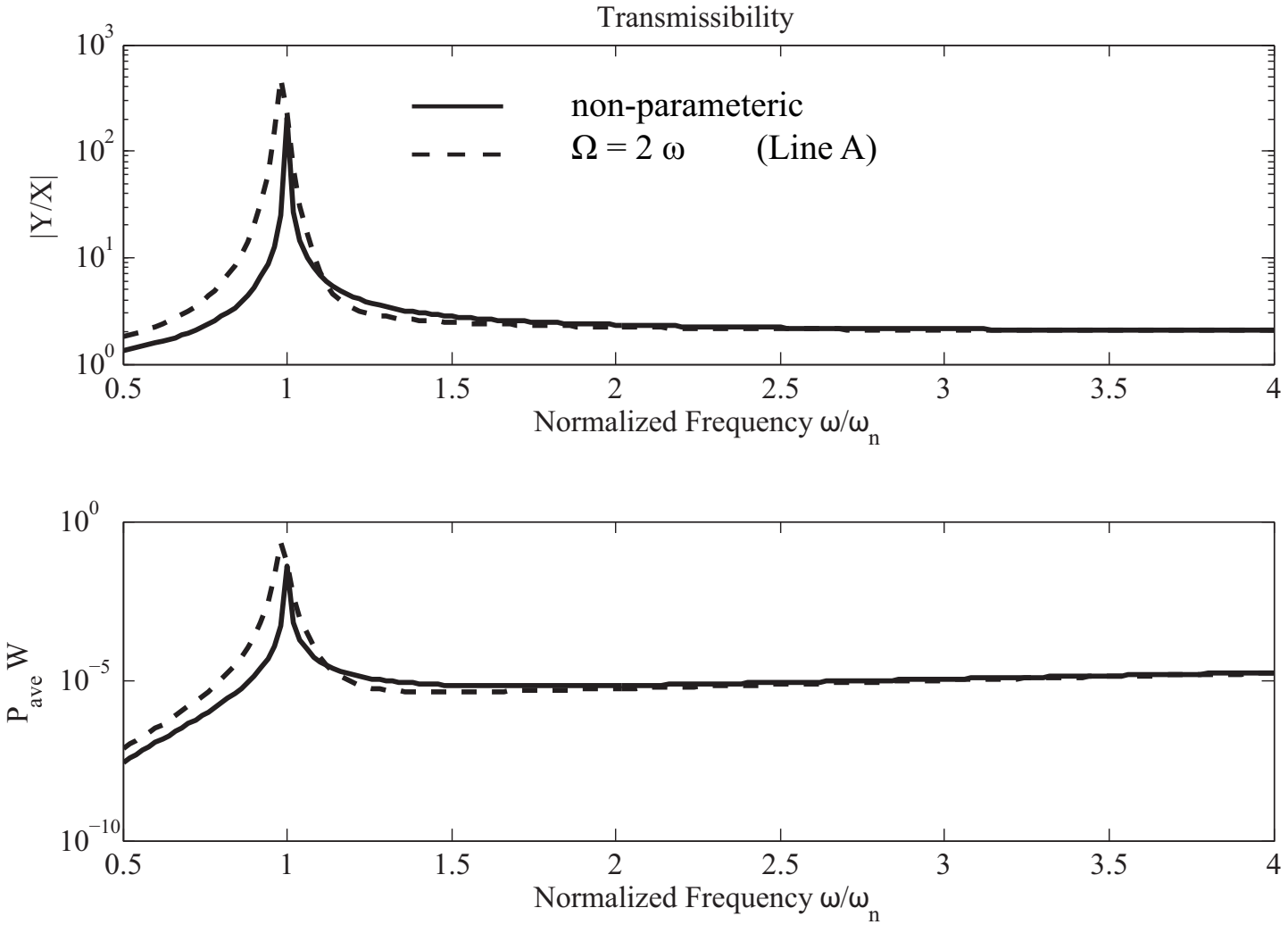

Analytical solutions of the non-parametric and parametric harvesters (B. Zaghari et al., 2014).

The effects of changing frequencies on power consumption

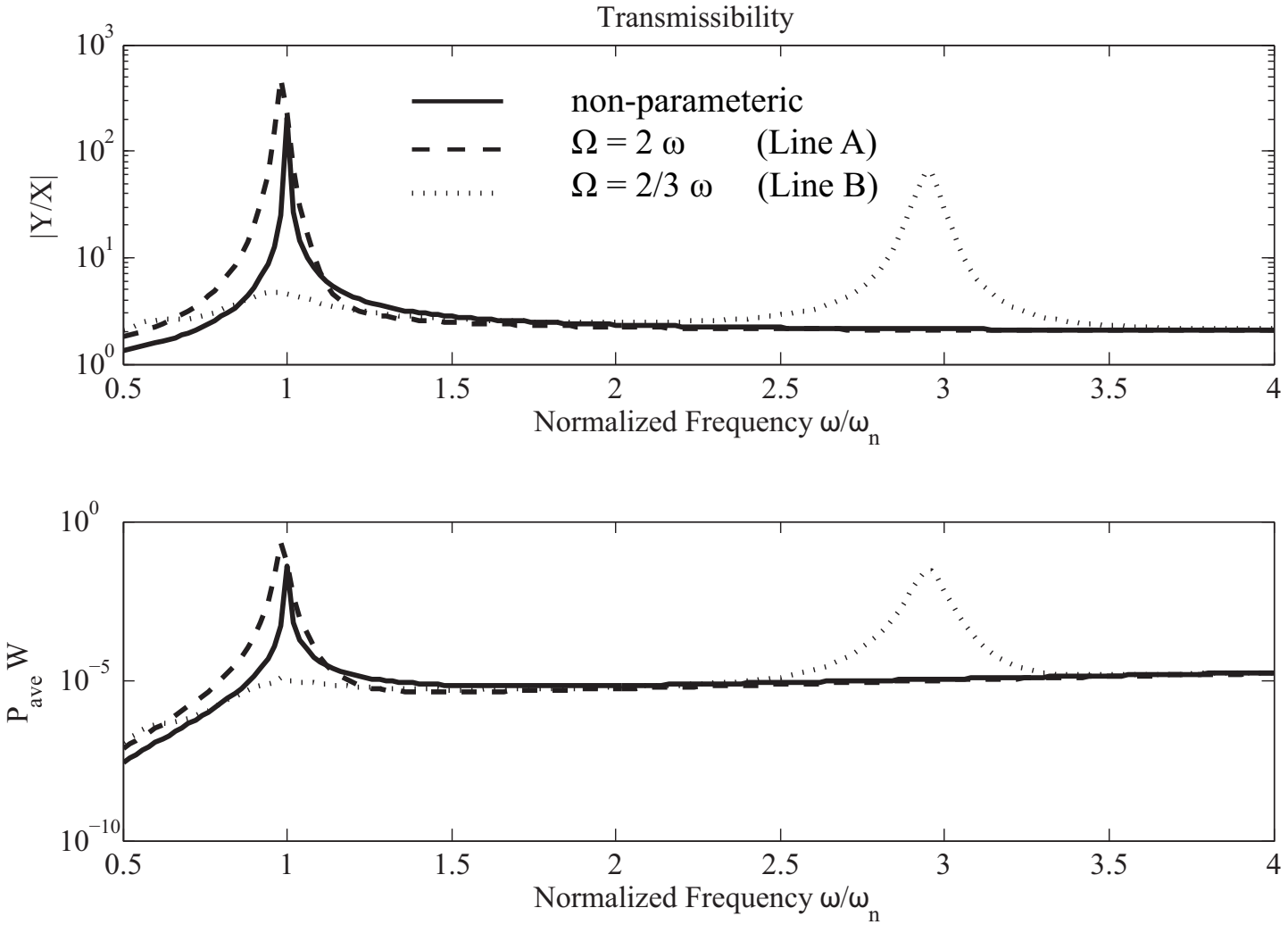

Analytical solutions of the non-parametric and parametric harvesters (B. Zaghari et al., 2014).

The effects of changing frequencies on power consumption

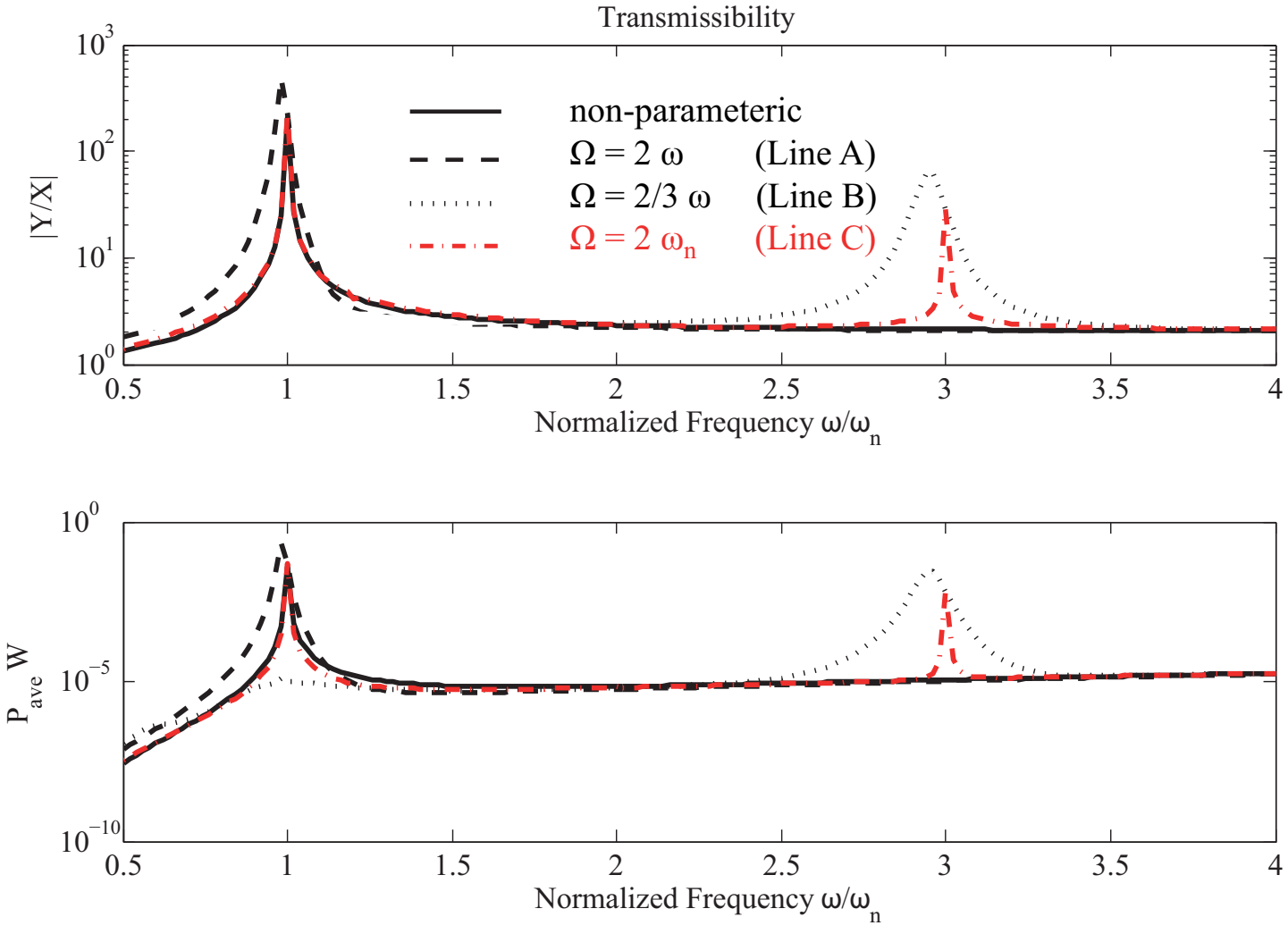

Analytical solutions of the non-parametric and parametric harvesters (B. Zaghari et al., 2014).

The effects of changing frequencies on power consumption

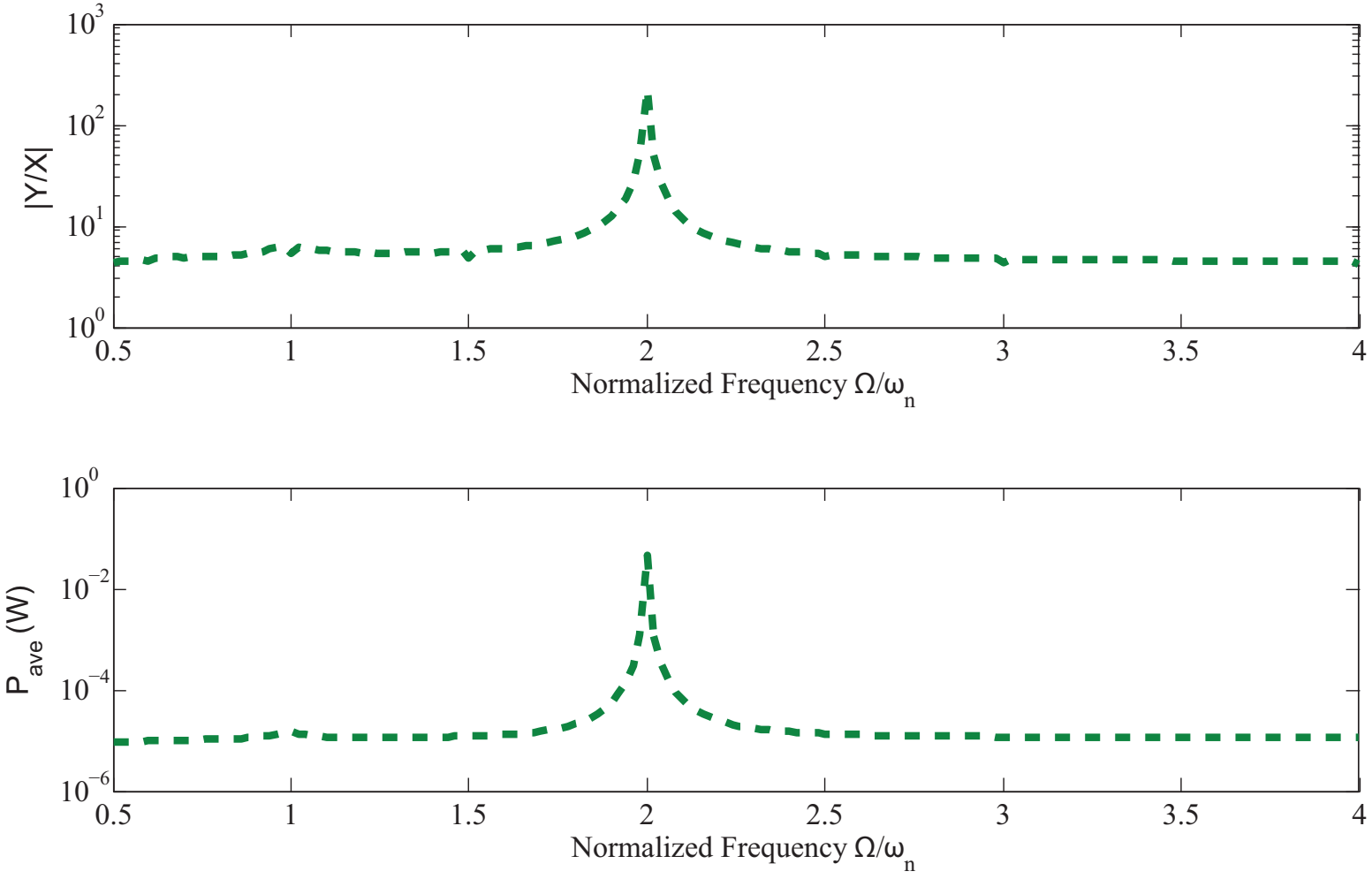

Analytical solution when Ω is changing and $\omega = \omega_n$ (B. Zaghari et al., 2014).

Amplitude a and phase φ of the system responses

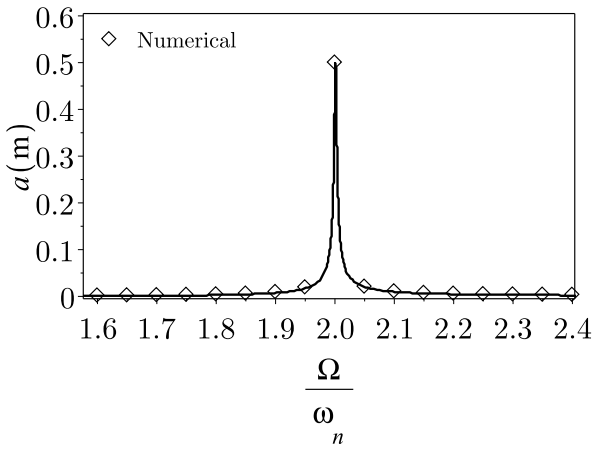

(a) Linear non-parametric

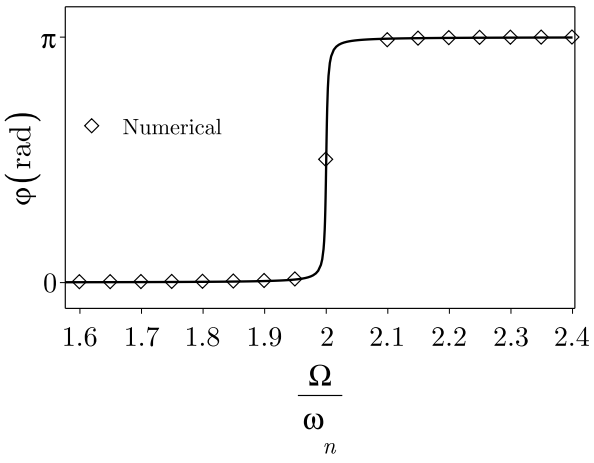

(b) Linear non-parametric

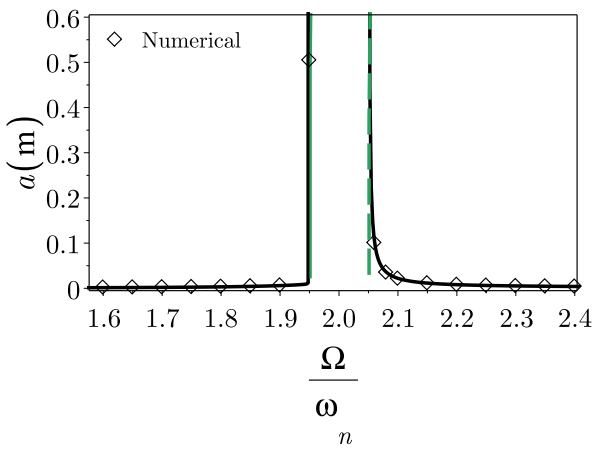

(c) Linear parametric, above the instability threshold

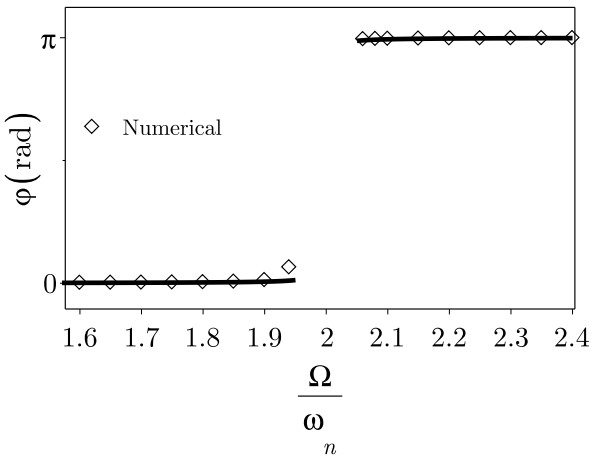

(d) Linear parametric, above the instability threshold

The effects of phase difference

The gain associated with the LPE system is

$$\text{Gain} = \frac{a\,|_{\delta \neq 0}}{a\,|_{\delta = 0}}. \tag{2}$$

This gain is calculated analytically from the amplitude of the steady-state response.

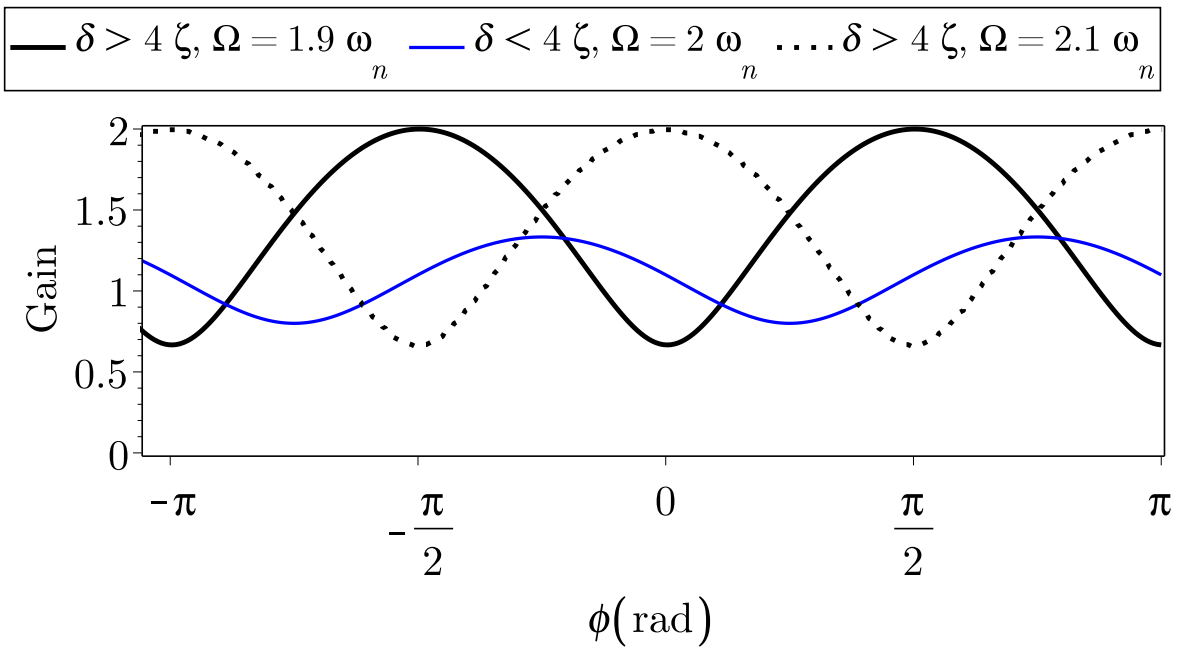

Gain versus base excitation phase difference ϕ for a linear parametrically excited system (B. Zaghari et al., 2016).

The effects of time-varying damping

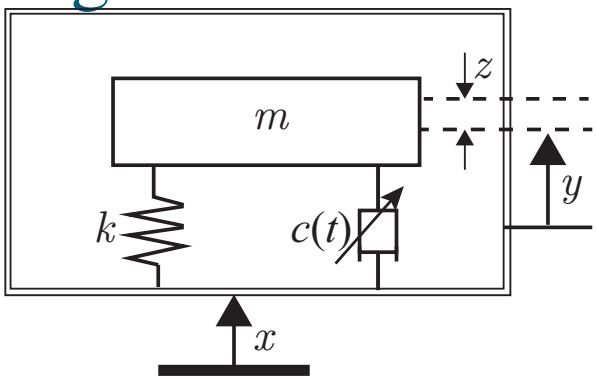

$$c(t) = c_0 + c_p \cos(\Omega t)$$

$$x = X \cos(\omega t)$$

Free vibration results, $x = 0$

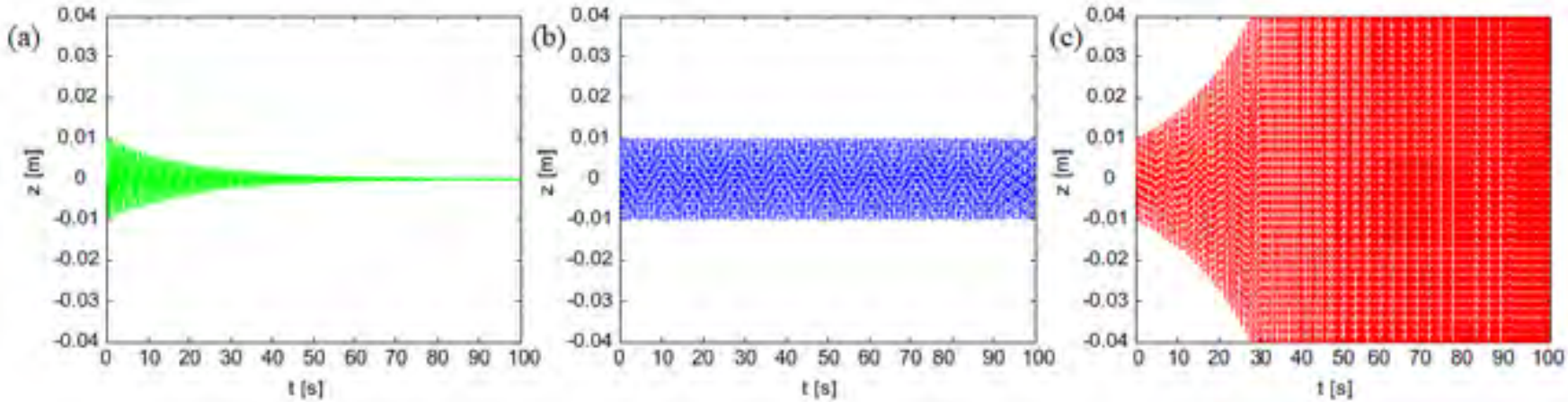

Relative displacement z of the system for different values of parametric damping (a) $c_p = -0.1c_0$, (b) $c_p = -c_0$, and (c) $c_p = -4c_0$ (M. Scapolan et al., 2017).

The effects of time-varying damping - base excited case

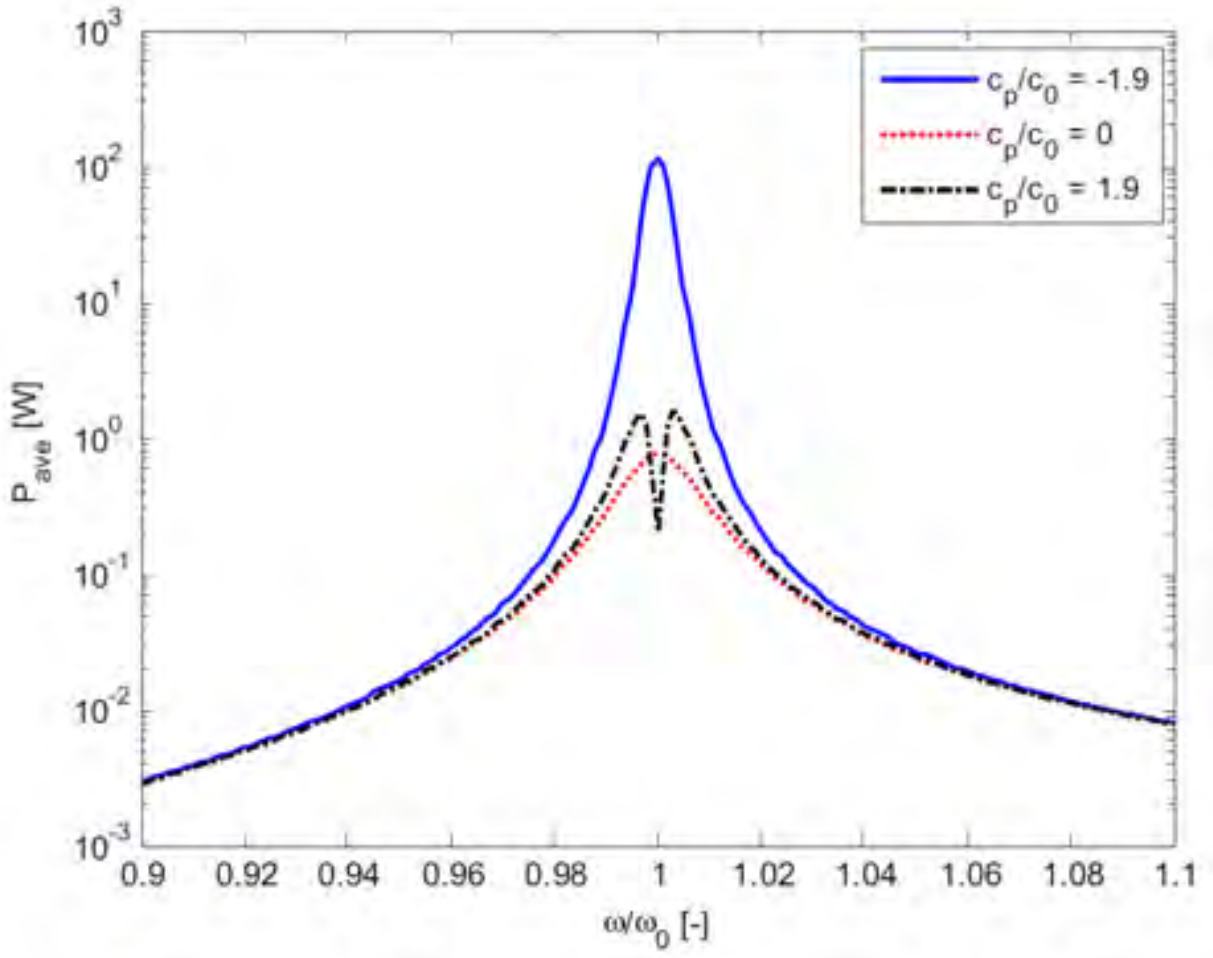

Average harvested power for parametric damping close to instability and non-parametric damping. ω and ω_0 are the base excitation and resonance frequency (M. Scapolan et al., 2017).

Nonlinearity in parametrically excited systems

Why nonlinearity?

- Real systems are nonlinear.
- Modern mechanical systems are more easily forced into a nonlinear regime.

Sources of nonlinearity:

- Geometrical
- Material
- Nonlinear forces
- Physical configuration

Electromagnetic system

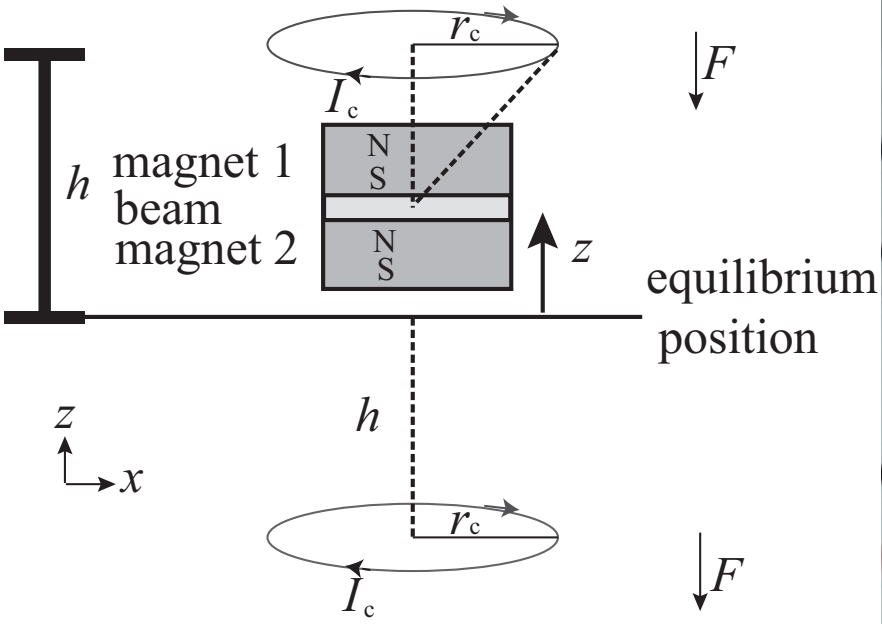

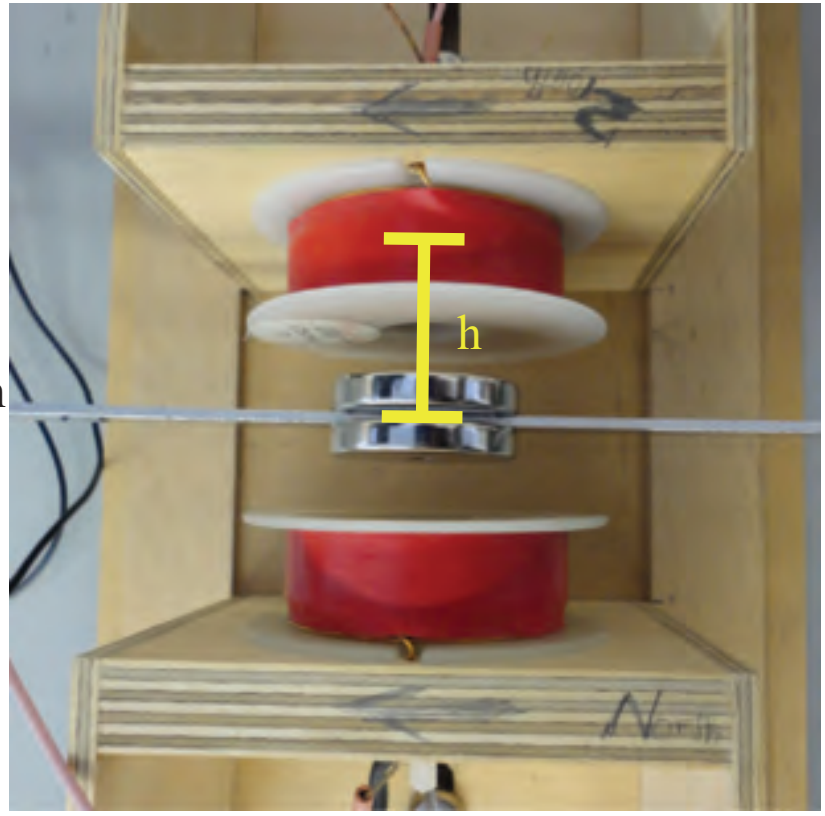

Electromagnetic forces generated by the current flow in coils are nonlinear forces and can influence the design of an electromagnetic energy harvester (B. Zaghari et al., 2018).

Nonlinear parametrically excited (NPE) system

$$\ddot{z} + 2\varepsilon\zeta\omega_n\dot{z} + \omega_n^2\left(1 + \varepsilon\,\delta\cos(\Omega t)\right)z + \omega_n^2\left(\varepsilon\,\alpha + \varepsilon\,\gamma\cos(\Omega t)\right)z^3 = 0$$

- parametric amplitude

Nonlinear parametrically excited (NPE) system

$$\ddot{z} + 2\varepsilon\zeta\omega_n\dot{z} + \omega_n^2\left(1 + \varepsilon\,\delta\cos(\Omega t)\right)z + \omega_n^2\left(\varepsilon\,\alpha + \varepsilon\,\gamma\cos(\Omega t)\right)z^3 = 0$$

- parametric amplitude
- cubic nonlinearity

Nonlinear parametrically excited (NPE) system

$$\ddot{z} + 2\varepsilon\zeta\omega_n\dot{z} + \omega_n^2\left(1 + \varepsilon\,\delta\cos(\Omega t)\right)z + \omega_n^2\left(\varepsilon\,\alpha + \varepsilon\,\gamma\cos(\Omega t)\right)z^3 = 0$$

- parametric amplitude
- cubic nonlinearity
- cubic parametric nonlinearity

Nonlinear parametrically excited (NPE) system

$$\ddot{z} + 2\varepsilon\zeta\omega_n\dot{z} + \omega_n^2\left(1 + \varepsilon\,\delta\cos(\Omega t)\right)z + \omega_n^2\left(\varepsilon\,\alpha + \varepsilon\,\gamma\cos(\Omega t)\right)z^3 = 0$$

- bookkeeping parameter

Stability and solutions of the nonlinear parametrically excited (NPE) system can be studied by:

- The second method of Lyapunov
- Methods of Harmonic Balance (HBM)
- Perturbation methods (Methods of Averaging, Multiple Scales, and Varying Amplitudes)

Effect of cubic stiffness nonlinearity

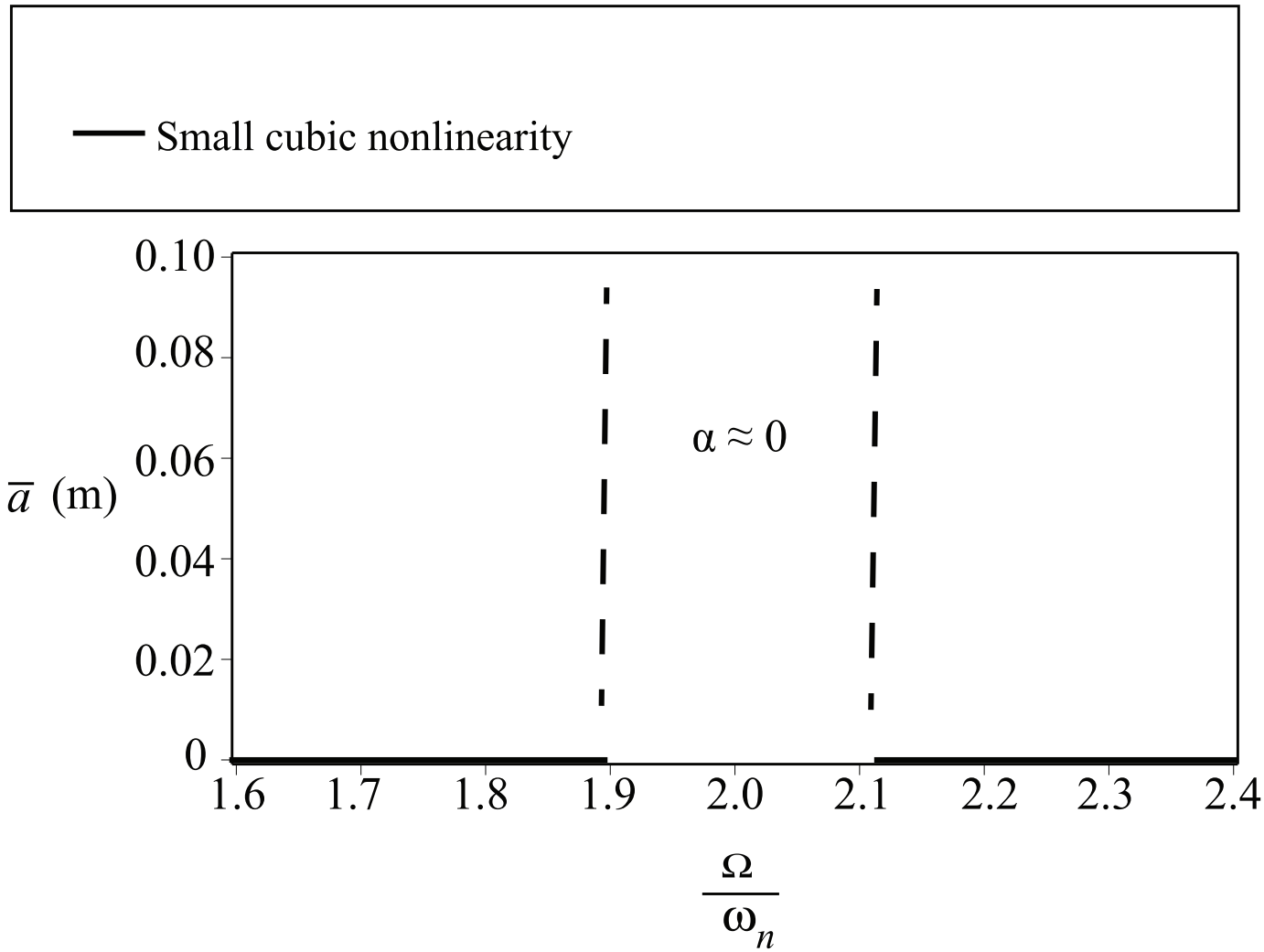

Analytical amplitude-frequency curves, $\varepsilon\alpha = 0.5\text{m}^{-2}$, $\varepsilon\delta = 0.25$, $\varepsilon\zeta = 0.03$, and $\varepsilon\gamma = 0$.

Hardening nonlinearity

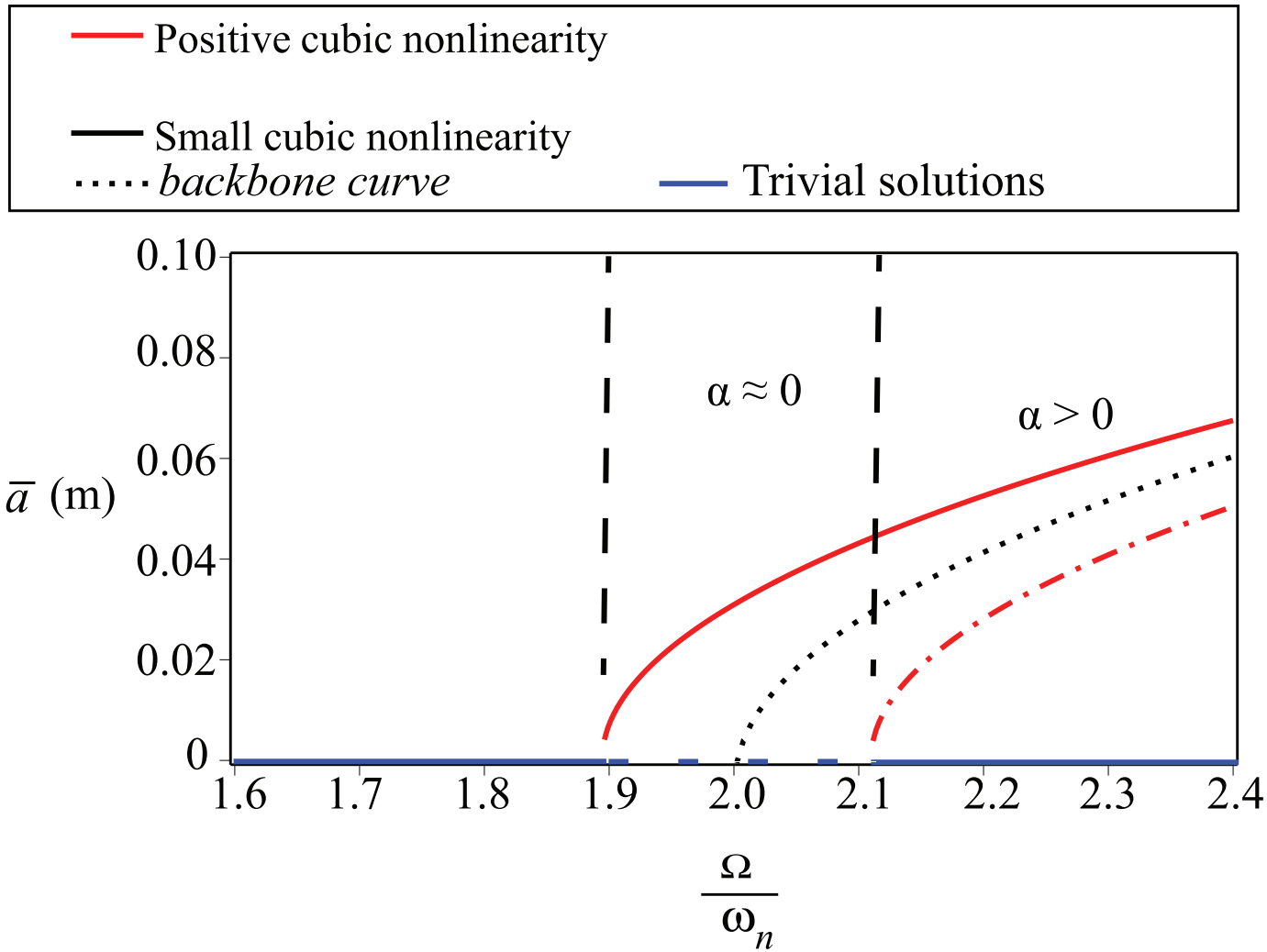

Analytical amplitude-frequency curves, $\varepsilon\alpha = 150\text{m}^{-2}$, $\varepsilon\delta = 0.25$, $\varepsilon\zeta = 0.03$, and $\varepsilon\gamma = 0$.

Softening nonlinearity

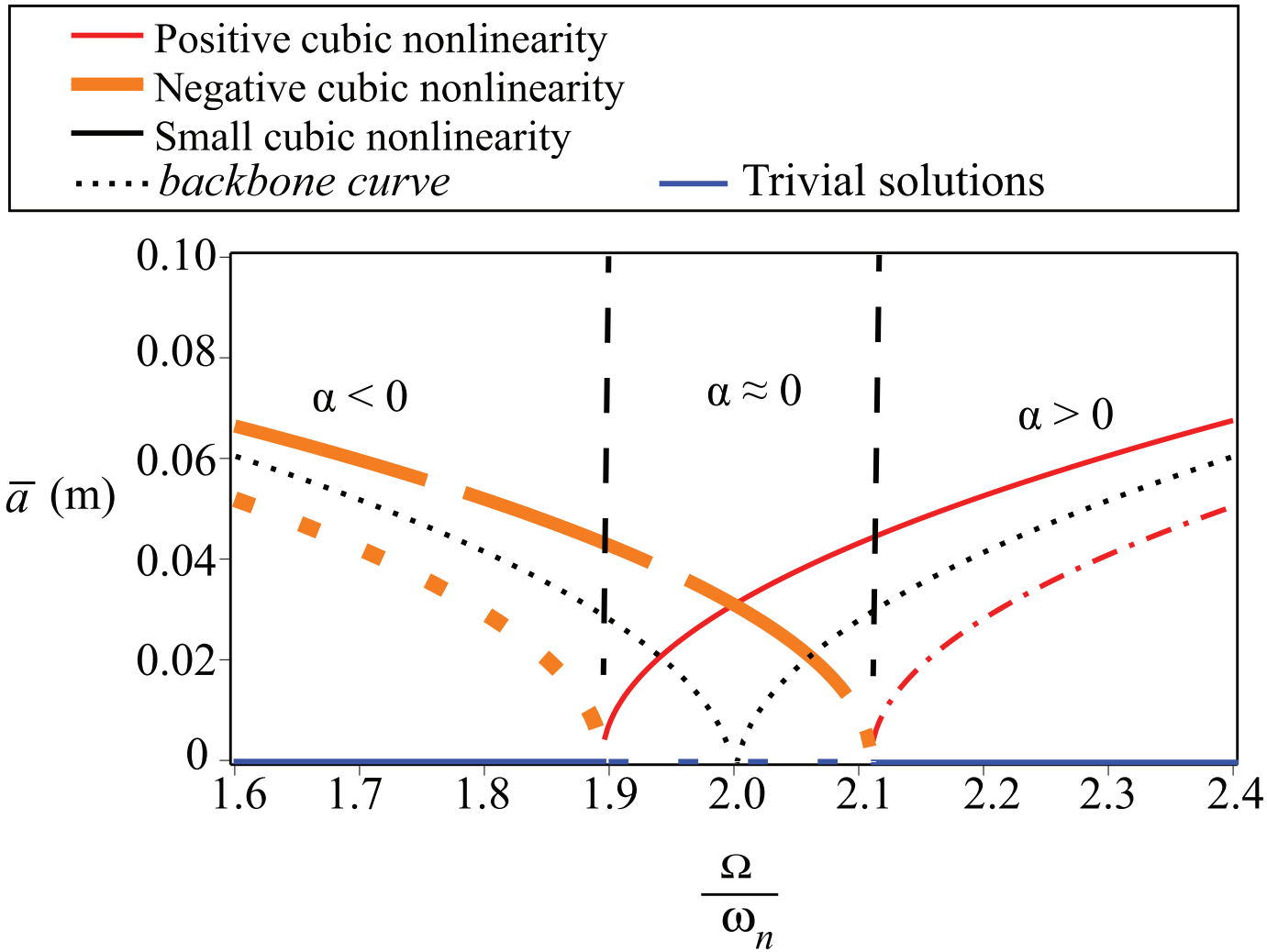

Analytical amplitude-frequency curves, $\varepsilon\alpha = -150\text{m}^{-2}$, $\varepsilon\delta = 0.25$, $\varepsilon\zeta = 0.03$, and $\varepsilon\gamma = 0$.

Frequency response plot for NPE

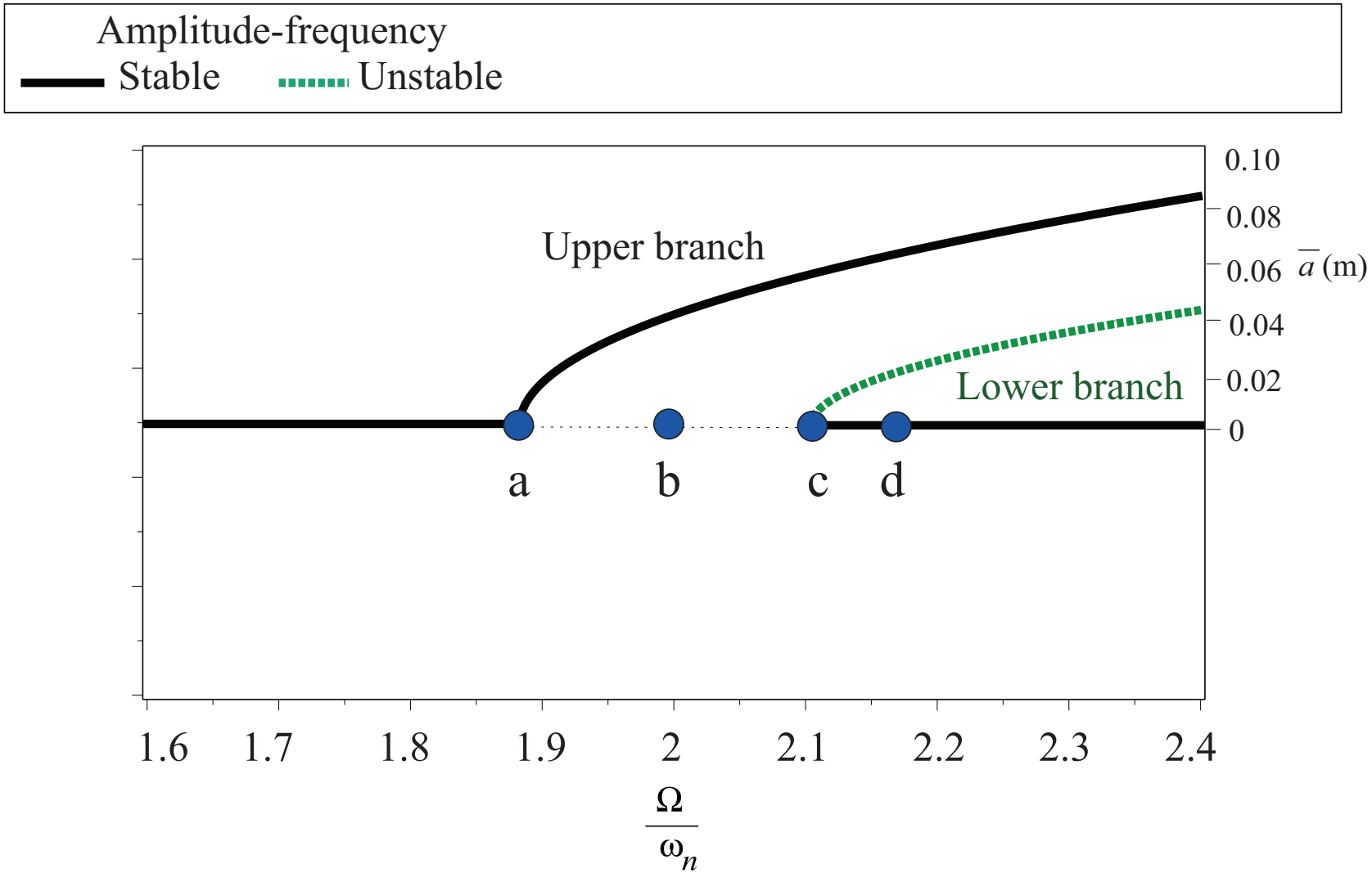

$\varepsilon\zeta = 0.03$, $\omega_n = 31.62\text{rads}^{-1}$, $\varepsilon\delta = 0.25$, $\varepsilon\alpha = 150\text{m}^{-2}$, and $\varepsilon\gamma = 80\text{m}^{-2}$.

Frequency response plot for NPE

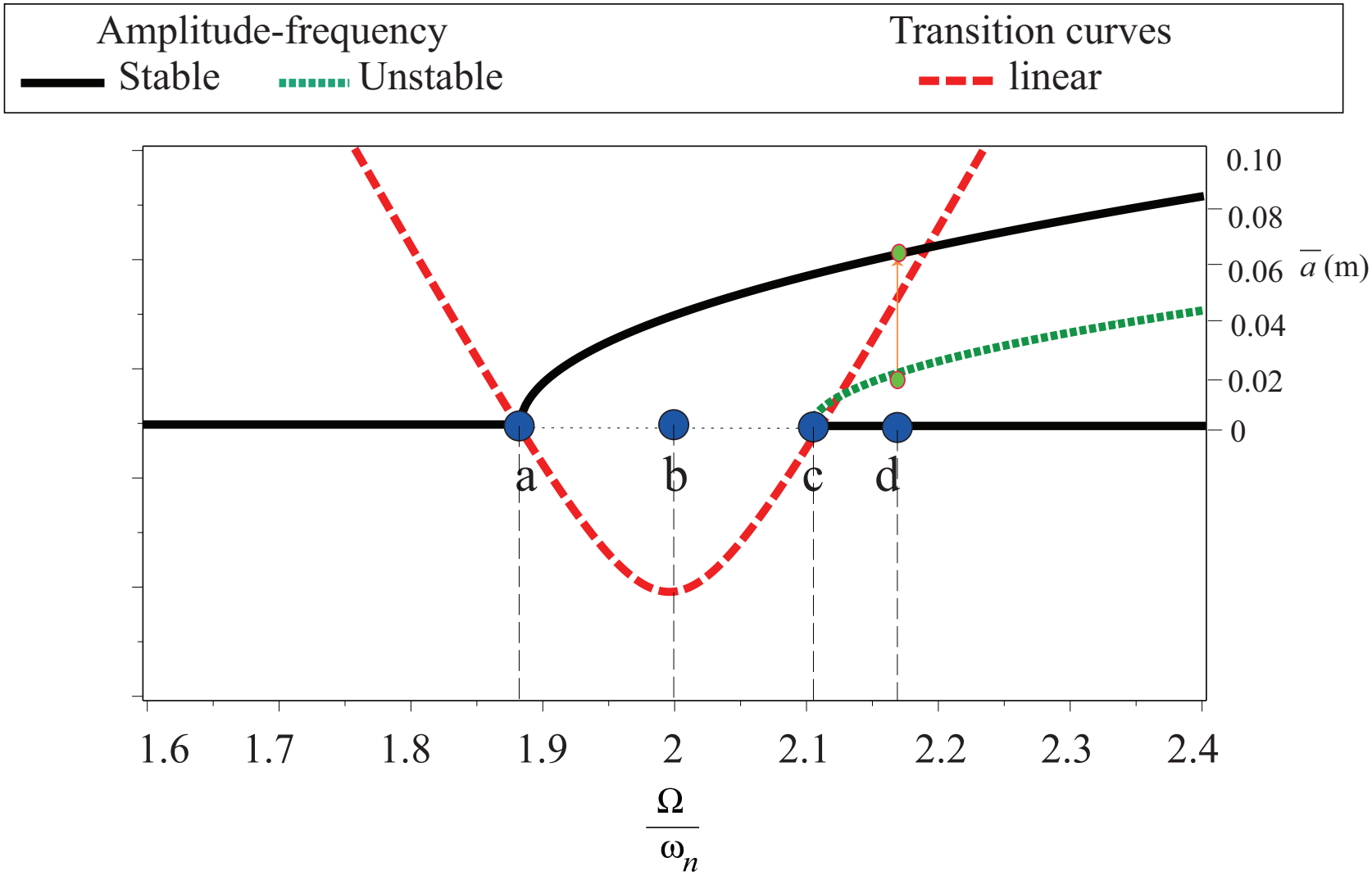

$\varepsilon\zeta = 0.03$, $\omega_n = 31.62\text{rads}^{-1}$, $\varepsilon\delta = 0.25$, $\varepsilon\alpha = 150\text{m}^{-2}$, and $\varepsilon\gamma = 80\text{m}^{-2}$.

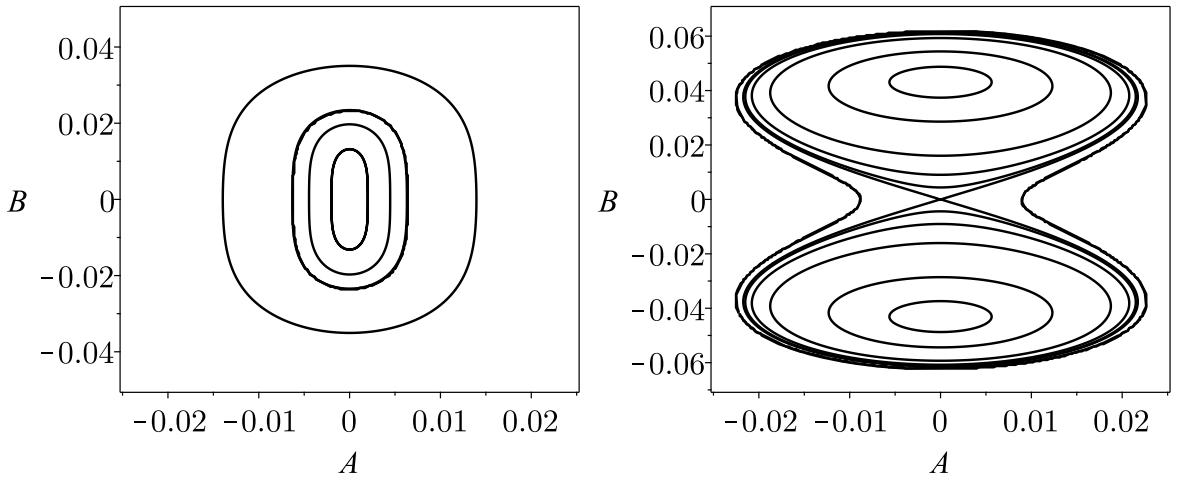

(a) (b)

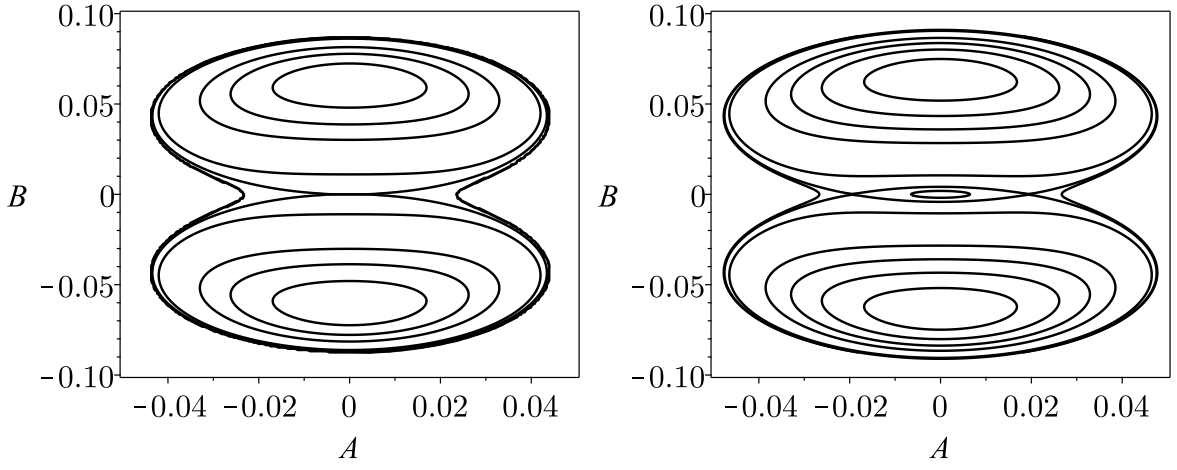

(c) (d)

The phase portraits correspond to different points on the transition curve when $\zeta = 0$ (B. Zaghari, 2016).

Conclusions

- Vibration energy harvesting research is not mature yet. Many research challenges still exist in applying the technology.
- The restrictions and limitations of real world environments must be continually designed around in order to create the best technology possible.
- Linear harvesters produce more energy in most applications where a clear characteristic frequency is present.
- Linear time-varying harvesters can increase the bandwidth and the power harvested.

Acknowledgement

Funding from EPSRC Platform Grant, Clean Sky, and EnABLES.

I would like to thank Prof. Steve Beeby, Prof. Neil White, Prof. Ling Wang, Dr. Alex Weddell, Dr. Emiliano Rustighi, Dr. Maryam Ghandchi Tehrani, Dr. Fadi Dohnal, and Prof. Subhash Sinha.

Thank you

These slides are available on GitHub at https://tinyurl.com/y9uwtz3q.